

NASA/TM—2008-215463



Long-Range Transhorizon Lunar Surface Radio Wave Propagation in the Presence of a Regolith and a Sparse Exospheric Plasma

Robert M. Manning
Glenn Research Center, Cleveland, Ohio

NASA STI Program . . . in Profile

Since its founding, NASA has been dedicated to the advancement of aeronautics and space science. The NASA Scientific and Technical Information (STI) program plays a key part in helping NASA maintain this important role.

The NASA STI Program operates under the auspices of the Agency Chief Information Officer. It collects, organizes, provides for archiving, and disseminates NASA's STI. The NASA STI program provides access to the NASA Aeronautics and Space Database and its public interface, the NASA Technical Reports Server, thus providing one of the largest collections of aeronautical and space science STI in the world. Results are published in both non-NASA channels and by NASA in the NASA STI Report Series, which includes the following report types:

- **TECHNICAL PUBLICATION.** Reports of completed research or a major significant phase of research that present the results of NASA programs and include extensive data or theoretical analysis. Includes compilations of significant scientific and technical data and information deemed to be of continuing reference value. NASA counterpart of peer-reviewed formal professional papers but has less stringent limitations on manuscript length and extent of graphic presentations.
- **TECHNICAL MEMORANDUM.** Scientific and technical findings that are preliminary or of specialized interest, e.g., quick release reports, working papers, and bibliographies that contain minimal annotation. Does not contain extensive analysis.
- **CONTRACTOR REPORT.** Scientific and technical findings by NASA-sponsored contractors and grantees.
- **CONFERENCE PUBLICATION.** Collected

papers from scientific and technical conferences, symposia, seminars, or other meetings sponsored or cosponsored by NASA.

- **SPECIAL PUBLICATION.** Scientific, technical, or historical information from NASA programs, projects, and missions, often concerned with subjects having substantial public interest.
- **TECHNICAL TRANSLATION.** English-language translations of foreign scientific and technical material pertinent to NASA's mission.

Specialized services also include creating custom thesauri, building customized databases, organizing and publishing research results.

For more information about the NASA STI program, see the following:

- Access the NASA STI program home page at <http://www.sti.nasa.gov>
- E-mail your question via the Internet to help@sti.nasa.gov
- Fax your question to the NASA STI Help Desk at 301-621-0134
- Telephone the NASA STI Help Desk at 301-621-0390
- Write to:
NASA Center for AeroSpace Information (CASI)
7115 Standard Drive
Hanover, MD 21076-1320

NASA/TM—2008-215463



Long-Range Transhorizon Lunar Surface Radio Wave Propagation in the Presence of a Regolith and a Sparse Exospheric Plasma

Robert M. Manning
Glenn Research Center, Cleveland, Ohio

National Aeronautics and
Space Administration

Glenn Research Center
Cleveland, Ohio 44135

October 2008

This report is a formal draft or working paper, intended to solicit comments and ideas from a technical peer group.

This report contains preliminary findings, subject to revision as analysis proceeds.

Level of Review: This material has been technically reviewed by technical management.

Available from

NASA Center for Aerospace Information
7115 Standard Drive
Hanover, MD 21076-1320

National Technical Information Service
5285 Port Royal Road
Springfield, VA 22161

Available electronically at <http://gltrs.grc.nasa.gov>

Long-Range Transhorizon Lunar Surface Radio Wave Propagation in the Presence of a Regolith and a Sparse Exospheric Plasma

Robert M. Manning
National Aeronautics and Space Administration
Glen Research Center
Cleveland, Ohio 44135

ABSTRACT

Long-range, over-the-horizon (transhorizon) radio wave propagation is considered for the case of the moon. In the event that relay satellites are not available or otherwise unwarranted for use, transhorizon communication provides for a contingency or backup option for non line-of-sight lunar surface exploration scenarios. Two potential low-frequency propagation mechanisms characteristic of the lunar landscape are the lunar regolith and the photoelectron induced plasma exosphere enveloping the moon. Although it was hoped that the regolith would provide for a spherical waveguide which could support a trapped surface wave phenomena, it is found that, in most cases, the regolith is deleterious to long range radio wave propagation. However, the presence of the plasma of the lunar exosphere supports wave propagation and, in fact, surpasses the attenuation of the regolith. Given the models of the regolith and exosphere adopted here, it is recommended that a frequency of 1 MHz be considered for low rate data transmission along the lunar surface. It is also recommended that further research be done to capture the descriptive physics of the regolith and the exospheric plasma so that a more complete model can be obtained.

This comprehensive theoretical study is based entirely on first principles and the mathematical techniques needed are developed as required; it is self-contained and should not require the use of outside resources for its understanding.

I. Introduction

The subject of this memorandum is a theoretical study of the possibility of long range electromagnetic wave propagation beyond the horizon (i.e., transhorizon) for purposes of contingency communications to support lunar surface exploration activities when the use of a relay satellite is not possible or warranted. For a source of radiation on or above the lunar surface, diffraction will of course be a mechanism for such transhorizon propagation as it is on the Earth. This effect is prevalent only at low radio frequencies in the KHz or low MHz range. Thus, lunar transhorizon propagation can only be considered at low frequencies and hence, low data rates. However, the lunar environment has the features that can also support long-range propagation.

The moon possesses two characteristic features that can potentially lend themselves to the support of transhorizon radio frequency propagation along its surface. First, the moon has a regolith [1], i.e., a thin fragmental layer of rock and minerals as well as glass, that covers all the rock formations on the moon. Its thickness subtends 10 meters to 100 meters below the surface; the thickness most likely varies along the surface especially near crater rims and mountain ranges. The source of the regolith is meteorite bombardment and related secondary processes as well as volcanic eruptions.

If the electrical characteristics of the regolith are sufficiently different than those of the core, the regolith has the potential to act as a spherical waveguide for low frequency electromagnetic radiation within which trapped surface waves or “whispering gallery” waves can travel to great distances along the surface.

In addition to the regolith, the moon also possesses an “ionosphere”, or more appropriately, an exosphere, a layer of electrons that is apparently formed by the liberation of electrons from the lunar surface by the solar wind. This photoelectron layer has been observed by the Apollo Lunar Science Experiment Package (ALSEP) [2] as well as by the Russian Luna 22 spacecraft [3]. It is important to note that this photoelectron layer is not a thermal ionospheric plasma like that of the Earth, which results from photoionization of neutral exospheric molecules [4]. As a result of the photoelectron source of the lunar exosphere, this phenomenon can only be expected to occur on the dayside of the moon

As will be displayed below, the charge density of the lunar exosphere begins at the surface and increases up to the height of 10 km after which it decreases again. In such a scenario, electromagnetic waves, with a source on the lunar surface, will not reflect beyond the horizon as in the case of the layered ionosphere of the Earth, but will again be guided around the surface of the moon as in the case of a dielectric waveguide of varying refractive index.

The purpose of this work is to theoretically study the effect of the lunar regolith as well as its exosphere plasma on low-frequency radio wave propagation. Thus, there are two propagation mechanisms that will be collectively studied to determine the potential of long-range, transhorizon radio wave transmission, i.e., that of the regolith and the contribution of the exosphere. Section II will detail the electrical properties of the regolith and the exosphere. In both cases, the properties have only been so far remotely obtained and can, over the course of future lunar exploration, change. The mathematical model of these propagation mechanisms will be kept general enough to accommodate the

evolution of the quantitative understanding of the regolith and exosphere. Section III will present the mathematical model of the lunar propagation environment. Propagation equations will be established for the three regions of the core, regolith, and the exosphere. These differential equations will then be solved by matching boundary conditions across the regions. Two cases will then be considered, i.e., the case where there is only a regolith with no exosphere and the case in which the exosphere is present. This exercise will allow for the development of the mathematical technique using the simpler case of just the regolith and, in addition, will allow one to isolate the effect of the regolith alone on transhorizon propagation. As far as mathematical technique is concerned, every effort is made to make this study self-contained and mathematical detail will not be spared. Two appendices are also provided to help with the rigor.

II. THE CORE, THE REGOLITH, AND THE EXOSPHERE

Figure 1 displays the model of the lunar propagation environment as envisioned in this work. Here, the Moon is modeled to possess a core (Region 1) of dielectric permittivity ϵ_1 followed by a very thin regolith (Region 2) of thickness δ and permittivity ϵ_2 ; both the core and regolith give rise to an overall lunar radius a .

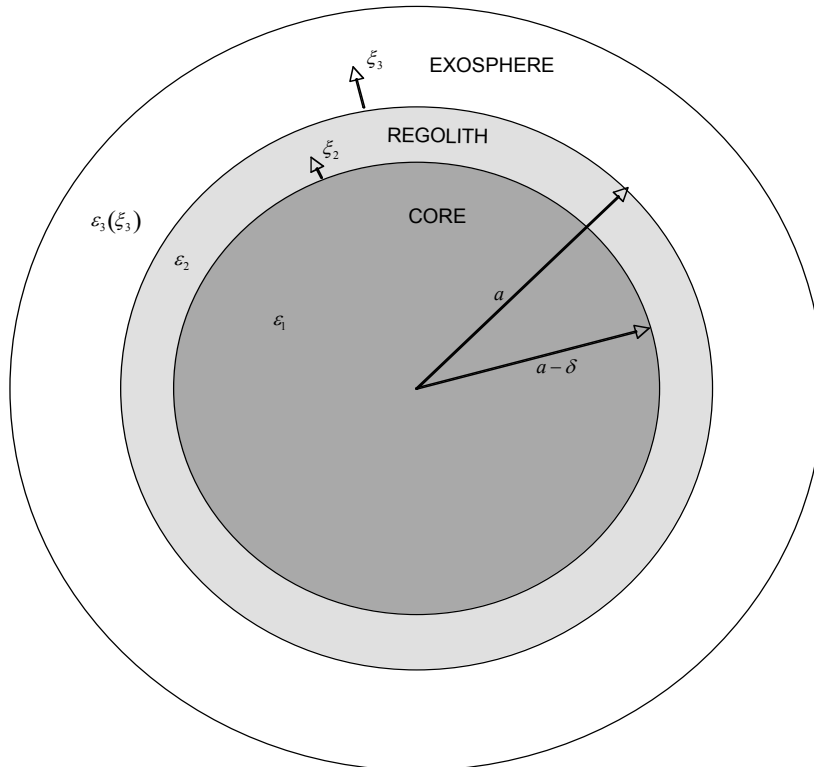


Figure 1. Defining the Propagation Regions of the Moon

Here, ξ_2 and ξ_3 are ‘local’ radial coordinates measured, respectively, from the surface of the core and the surface of the regolith. Later, a spherical coordinate system will be introduced in which the radial coordinate of which will be reckoned to the center of the moon.

The outer surface of the Moon is taken to have an exosphere (Region 3). The electron concentration profile within this region gives rise to a tenuous plasma of permittivity profile $\varepsilon_3(\xi_3)$.

a. Permittivity and Conductivity of the Core and Regolith

A majority of the electrical characteristics of the core and regolith are, of course, indirectly obtained [5,6] and their estimates seem to vary. In a related investigation [7], the moon is taken to have a regolith that subtends the first 100 meters below the surface, after which the core is reached. However, as mentioned above, some studies indicate that the regolith thickness can be a minimum of 10 m. In this study, two values for the thickness of the regolith will be considered, viz., $\delta = 50$ m and $\delta = 100$ m. The permittivity of the core is taken [7] to be within the range from $\varepsilon_1 = 5$ to $\varepsilon_1 = 10$ with an associated conductivity within the range from $\sigma_1 = 10^{-4}$ mhos/m to $\sigma_1 = 10^{-3}$ mhos/m. Similarly, the regolith region is characterized [7] by a permittivity range from $\varepsilon_2 = 2$ to $\varepsilon_2 = 3$ and a conductivity range from $\sigma_2 = 10^{-6}$ mhos/m to $\sigma_2 = 10^{-5}$ mhos/m. For the purposes of the present investigation, the values of the relevant parameters are taken as displayed in Table 1.

REGION	PERMITTIVITY	CONDUCTIVITY
Core	$\varepsilon_1 = 5$	$\sigma_1 = 5 * 10^{-4}$ mhos/m
Regolith ($\delta = 50$ m, $\delta = 100$ m)	$\varepsilon_2 = 3$	$\sigma_2 = 5 * 10^{-6}$ mhos/m

Table 1. Electrical Parameters of the Moon

b. Permittivity and Conductivity of the Exosphere

As mentioned above, the lunar exosphere has been experimentally observed [3], the properties of which are shown in Figure 2 which displays the height profile of the electron concentration of the lunar exosphere. As can be seen from the figure, the electron concentration has a maximum $N_m = 1000 \text{ cm}^{-3}$ occurring at the height $\xi_{30} = 10$ km. Here, ξ_3 is the ‘local’ coordinate measured from the lunar surface, as shown in Fig.1. The electron concentration profile of the exosphere is most easily modeled as a parabolic profile with its apex at $\xi_3 = \xi_{30}$.

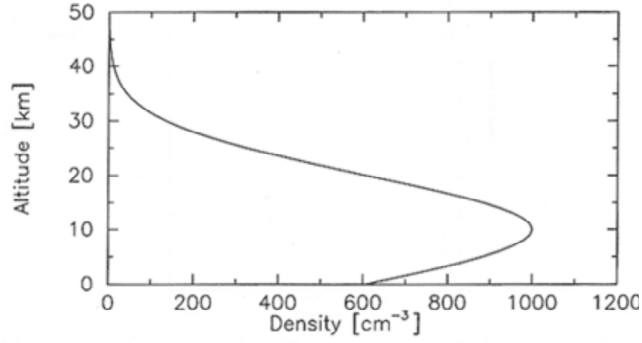


Figure 2. Electron Concentration Profile of Lunar Exosphere

Thus, letting η be a constant, one can write for this concentration

$$N(\xi_3) = N_m - \eta(\xi_3 - \xi_{30})^2 \quad (1)$$

This constant is determined from the fact that the concentration at the surface $N(0)$ is given, by Eq.(1) as

$$N(0) = N_m - \eta(\xi_{30})^2 \quad (2)$$

Hence, $\eta = \Delta N / \xi_{30}^2$ where $\Delta N \equiv N_m - N(0)$. From Fig.2, the differential concentration of the electrons is $\Delta N = 400 \text{ cm}^{-3}$. Thus, the model for the electron concentration profile of the lunar ionosphere is given by

$$N(\xi_3) = N_m - \Delta N \left(\frac{\xi_3 - \xi_{30}}{\xi_{30}} \right)^2 \quad (3)$$

The associated permittivity profile of this ‘parabolic’ exosphere is found by applying a well-known model for free electron plasma behavior in an electric field [8] with $e^{-i\omega t}$ time dependence that gives

$$\varepsilon_3(\xi_3) = 1 - \frac{4\pi e^2 N(\xi_3)}{m\omega(\omega + i\nu_{eff})} \quad (4)$$

where e and m are, respectively, the charge and mass of an electron, ω is the angular frequency of the electromagnetic radiation and ν_{eff} is the effective collision frequency for the electrons. This equation can be re-written as

$$\varepsilon_3(\xi_3) = 1 - \frac{4\pi e^2 N(\xi_3)}{m(\omega^2 + \nu_{eff}^2)} + i \frac{4\pi}{\omega} \sigma_3(\xi_3) \quad (5)$$

where

$$\sigma_3(\xi_3) = \frac{e^2 \nu_{eff} N(\xi_3)}{m(\omega^2 + \nu_{eff}^2)} \quad (6)$$

is the conductivity of the exosphere plasma. However, in a tenuous plasma as is represented by Fig.2, one has that $\nu_{eff} \approx 0$ thus rendering the plasma conductivity zero and allowing Eq.(5), after substitution of Eq.(3) to be written as

$$\varepsilon_3(\xi_3) = \varepsilon_{30} + \varepsilon_{3\Delta} \left(\frac{\xi_3 - \xi_{30}}{\xi_{30}} \right)^2 \quad (7)$$

where

$$\varepsilon_{30} \equiv 1 - \frac{4\pi e^2 N_m}{m\omega^2}, \quad \varepsilon_{3\Delta} \equiv \frac{4\pi e^2 \Delta N}{m\omega^2} \quad (8)$$

Equations (7) and (8) constitute the permittivity model of the lunar exosphere.

Using the values of the parameters quoted above in the text as well as $m = 9.1 \times 10^{-28}$ g and $e = 4.8 \times 10^{-10}$ esu, Eq.(7) for $\xi_3 = 0$ is plotted versus the operating frequency as is shown in Fig. 3. The graph clearly shows that at frequencies below 220 KHz, electromagnetic radiation does not propagate at the surface; this is the characteristic plasma frequency for the plasma at the surface. Only frequencies above this threshold can be transmitted along the lunar surface characterized by the profile of Fig. 2. Figure 4 displays the behavior of the exospheric permittivity as a function of height above the surface at a frequency of 500 KHz. A minimum exists at the characteristic height ξ_{30} . This interesting circumstance suggests that a ‘trough’ exists in the permittivity distribution along which electromagnetic waves may be guided in to a transhorizon location.

Now that the regions of propagation have been identified and their prevailing parameter values been established, one can now begin to model the electromagnetic propagation behavior of these regions and how they all couple to contribute to long range transhorizon transmission.

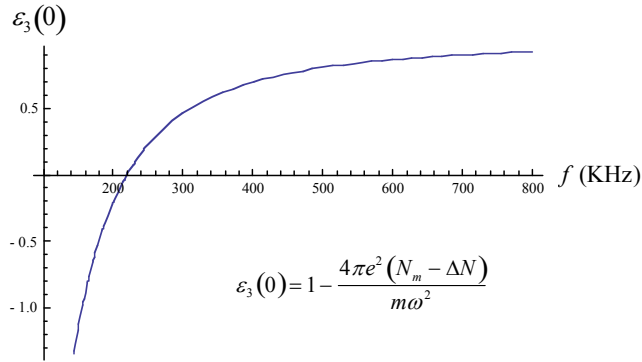


Figure 3. Permittivity of Exosphere vs. Operating Frequency

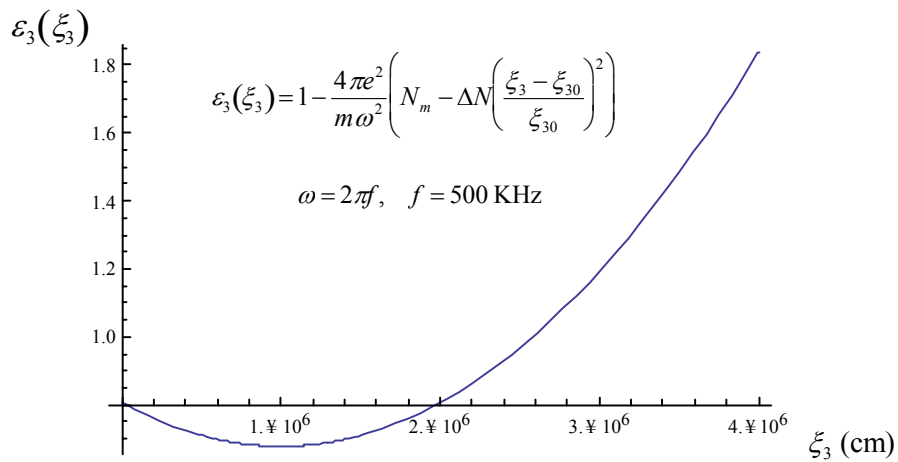


Figure 4. Permittivity of Exosphere vs. Height at 500 KHz

III. MODELING OF THE LUNAR PROPAGATION ENVIRONMENT

a. Derivation of the Propagation Equations for the Three Regions

As introduced above, the lunar propagation scenario is as depicted in Figure 1. There are three electrically disparate regions defined by the core (region 1), the regolith (region 2), and the exosphere (region 3). The spherical symmetry of the situation naturally suggests that one consider a spherical coordinate (r, θ, ϕ) system be attached to the moon, the center of which is placed at the center of the moon. Here, r is the radial

distance from the center, θ is the colatitude, as reckoned from a polar axis which is taken to be along the source of the electromagnetic radiation placed on the surface, and ϕ is the azimuthal angle. The source is taken to be a vertical electric dipole placed at a distance r_s from the surface within region 3; such a source radiates transverse magnetic (TM) waves. Regions 2 and 3 are also characterized by the distances above their respective surfaces. Taking the radius of the moon to be a and the thickness of the regolith to be δ , region 2 is defined by the radial coordinate ξ_2 where $a - \delta \leq \xi_2 < a$. Similarly, region three is defined by the radial coordinate ξ_3 where $a \leq \xi_3$.

The modeling approach must necessarily be based on the Maxwell equations that govern the behavior and the dynamics of the electromagnetic field. So as not to deter from the presentation of the subject matter, the Maxwell equations as well as their solution in terms of a scalar potential for TM electromagnetic waves is given in Appendix A. There, it is shown that the field components of such a wave, with fields that are independent of the azimuthal coordinate ϕ , are given by

$$E_r = -\frac{1}{r \sin \theta} \frac{\partial}{\partial \theta} \left(\sin \theta \frac{\partial U_e}{\partial \theta} \right) \quad (9)$$

for the radial component of the electric field,

$$E_\theta(r, \theta) = \frac{1}{r} \frac{\partial}{\partial r} \left(r \frac{\partial U_e(r, \theta)}{\partial \theta} \right) \quad (10)$$

for the colatitude field component and

$$H_\phi(r, \theta) = +ik_0 n^2 \frac{\partial U_e(r, \theta)}{\partial \theta} \quad (11)$$

for the azimuthal component of the magnetic field, where $n^2 = \epsilon$ is the refractive index of the region in question. Here, $U_e(r, \theta)$ is the scalar potential for TM waves given by the solution of

$$\frac{1}{r} \frac{\partial^2}{\partial r^2} (r U_e) + \left(\frac{1}{r^2 \sin \theta} \right) \frac{\partial}{\partial \theta} \left(\sin \theta \frac{\partial U_e}{\partial \theta} \right) + \left(\frac{1}{r^2 \sin^2 \theta} \right) \left(\frac{\partial^2 U_e}{\partial \phi^2} \right) + k^2 U_e = 0 \quad (12)$$

Again, so as not to deter from the present discussion, the method of solution of Eq.(12) is presented in Appendix B in addition to its preferred form. Thus, the solution to Eq.(12) is taken to be of the form

$$U_e = U_e(r, \theta) = A \frac{\tilde{R}_l(r)}{r} P_l(-\cos \theta) \quad (13)$$

where $P_l(-\cos\theta)$ is the l^{th} order Legendre polynomial in the argument $-\cos\theta$ (See Appendix B for an explanation of this choice rather than using the traditional $+\cos\theta$.) and $\tilde{R}_l(r)$ is given by the solution of

$$\frac{d^2\tilde{R}_l(r)}{dr^2} + \left(k^2 - \frac{l(l+1)}{r^2}\right)\tilde{R}_l(r) = 0 \quad (14)$$

where $k \equiv \sqrt{\varepsilon}k_0$ is the wavenumber in the region defined by the permittivity ε and $k_0 \equiv 2\pi/\lambda$ is the free-space wavenumber for electromagnetic radiation of wavelength λ .

The function $P_l(-\cos\theta)$ is only a function of the colatitude and is therefore independent of which of the three regions is being considered. However, the radial component $\tilde{R}_l(r)$ of the scalar potential is indeed a function of the region through the wavenumber parameter k . Thus, there are three separate versions of Eq.(14) that must be considered, viz.,

$$\frac{d^2\tilde{R}_{l_1}(r)}{dr^2} + \left(k_1^2 - \frac{l(l+1)}{r^2}\right)\tilde{R}_{l_1}(r) = 0, \quad k_1^2 = \varepsilon_1 k_0^2, \quad 0 \leq r < a - \delta \quad (15)$$

for region 1 (the core),

$$\frac{d^2\tilde{R}_{l_2}(r)}{dr^2} + \left(k_2^2 - \frac{l(l+1)}{r^2}\right)\tilde{R}_{l_2}(r) = 0, \quad k_2^2 = \varepsilon_2 k_0^2, \quad a - \delta \leq r < a \quad (16)$$

for region 2 (the regolith), and

$$\frac{d^2\tilde{R}_{l_3}(r)}{dr^2} + \left(k_3^2(\xi_3) - \frac{l(l+1)}{r^2}\right)\tilde{R}_{l_3}(r) = 0, \quad k_3^2(\xi_3) = \varepsilon_3(\xi_3)k_0^2, \quad a \leq r, \quad \xi_3 = r - a \quad (17)$$

for region 3 (the exosphere).

b. Solution for Region 1

One must first consider the field distribution within the core region; this will then be used to calculate the impedance boundary condition at $r = a - \delta$ to which the fields within the regolith can be connected. To this end, consider the solution [9] of Eq.(15) for the scalar potential within the lunar core

$$\tilde{R}_{l_1}(r) = r[A_l j_l(k_1 r) + B_l n_l(k_1 r)], \quad r \leq a - \delta \quad (18)$$

where $j_l(k_1 r)$ and $n_l(k_1 r)$ are spherical Bessel functions given by

$$j_l(x) = \sqrt{\frac{\pi}{2x}} J_{l+1/2}(x), \quad n_l(x) = \sqrt{\frac{\pi}{2x}} N_{l+1/2}(x) \quad (19)$$

in terms of the Bessel function of the first kind $J_{n+1/2}(x)$ and the Bessel function of the second kind $N_{n+1/2}(x)$ (Neumann function). Hence, Eq.(13) becomes, for the core region,

$$U_{e_1}(r, \theta) = [A_1 j_l(k_1 r) + B_1 n_l(k_1 r)] P_l(-\cos \theta) \quad (20)$$

However, due to the properties of the functions $j_l(x)$ and $n_l(x)$, for the solution $U_{e_1}(r, \theta)$ to be finite at $r = 0$, one must have $B_1 = 0$,

$$U_{e_1}(r, \theta) = A_1 j_l(k_1 r) P_l(-\cos \theta) \quad (21)$$

The ‘matching’ of the solutions within region 1 and those of region 2 which is to follow, will be done through the use of the surface impedance at $r = a - \delta$. This impedance is defined by

$$Z_1 \equiv - \frac{E_{\theta_1}(r, \theta)}{H_{\phi_1}(r, \theta)} \Big|_{r=a_R} \quad (22)$$

where $a_R \equiv a - \delta$. From Eqs.(10) and (11),

$$E_{\theta_1}(r, \theta) = \frac{1}{r} \frac{\partial}{\partial r} \left(r \frac{\partial U_{e_1}(r, \theta)}{\partial \theta} \right) \quad (23)$$

$$H_{\phi_1}(r, \theta) = +ik_0 n_1^2 \frac{\partial U_{e_1}(r, \theta)}{\partial \theta}, \quad n_1^2 = \epsilon_1 \quad (24)$$

The use of the impedance concept of Eq.(22) is tantamount to employing the continuity boundary conditions of Eqs.(A48) and (A50) of Appendix A. Thus, substituting Eq.(21) into Eqs.(23) and (24) gives

$$E_{\theta_1}(r, \theta) = \frac{A_1}{r} \left[j_l(k_1 r) + r \frac{\partial j_l(k_1 r)}{\partial \theta} \right] \frac{\partial P_l(-\cos \theta)}{\partial \theta} \quad (25)$$

$$H_{\phi_1}(r, \theta) = +ik_0 n_1^2 A_1 j_l(k_1 r) \frac{\partial P_l(-\cos \theta)}{\partial \theta} \quad (26)$$

Using these expressions in Eq.(22) yields

$$Z_1 = + \left(\frac{i}{k_0 \epsilon_1} \right) \left[\frac{1}{a_R} + \frac{1}{j_l(k_1 r)} \frac{\partial j_l(k_1 r)}{\partial r} \right]_{r=a_R}$$

$$\approx + \left(\frac{i}{k_0 \epsilon_1} \right) \frac{1}{j_l(k_1 r)} \frac{\partial j_l(k_1 r)}{\partial r} \Big|_{r=a_R} \quad (27)$$

The evaluation of $j_l(k_1 r)$ at $r = a_R \gg 1$ requires asymptotic expansions of this function which can become rather unwieldy. However, one can adopt the method of [10] and consider the solution to the asymptotic form of the original equation, Eq.(15) with $r = a_R$. What one does in essence is to assume a thin shell about the radius a_R . To this end, Eq.(15) is approximately written

$$\frac{d^2 \tilde{R}_{l_1}}{d^2 r} + \left(k_1^2 - \frac{l(l+1)}{a_R^2} \right) \tilde{R}_{l_1} = 0 \quad (28)$$

the solution of which is

$$\tilde{R}_{l_1}(r) = A_1 e^{+i\kappa_{l_1} r} + B_1 e^{-i\kappa_{l_1} r}, \quad \kappa_{l_1} \equiv \left(k_1^2 - \frac{l(l+1)}{a_R^2} \right)^{1/2} \quad (29)$$

Equating this result with that of Eq.(18), and letting $B_1 = 0$ as before, gives the approximation

$$j_l(k_1 r) \approx A_1 \frac{e^{+i\kappa_{l_1} r}}{a_R^2} \quad (30)$$

Hence, using this approximation in Eq.(27), one has for the surface impedance at $r = a_R \equiv a - \delta$,

$$Z_1 = - \frac{1}{\epsilon_1^{1/2}} \left(1 - \frac{l(l+1)}{k_1^2 a_R^2} \right)^{1/2} \quad (31)$$

The modal value of the combination $l(l+1)$ will be determined by the behavior of the radial equation for region 2.

c. Solution for Region 2

Consider now the scalar potential within the regolith, region 2. One thus has from Eq.(16) and the coordinate geometry depicted in Fig. 1

$$\frac{d^2 \tilde{R}_{l_2}(r)}{dr^2} + \left(k_2^2 - \frac{l(l+1)}{r^2} \right) \tilde{R}_{l_2}(r) = 0, \quad k_2^2 = \varepsilon_2 k_0^2, \quad a - \delta \leq r < a \quad (32)$$

where

$$r = \xi_2 + (a - \delta) = \xi_2 + a_R \quad (33)$$

Using Eq.(33) in Eq.(32) and changing variables from r to ξ_2 gives

$$\frac{d^2 \tilde{R}_{l_2}(r)}{d\xi_2^2} + \left(k_2^2 - \frac{l(l+1)}{(\xi_2 + a_R)^2} \right) \tilde{R}_{l_2}(r) = 0 \quad (34)$$

Since the condition $\xi_2 \ll a_R$ prevails, one can follow the example given in Appendix B and expand the denominator of the second term within the parenthesis, viz.,

$$(\xi_2 + a_R)^{-2} = a_R^{-2} \left(1 + \frac{\xi_2}{a_R} \right)^{-2} \approx a_R^{-2} \left(1 - 2 \frac{\xi_2}{a_R} \right) \quad (35)$$

thus allowing Eq.(34) to be written as

$$\frac{d^2 \tilde{R}_{l_2}(r)}{d\xi_2^2} + \left(k_2^2 - \frac{l(l+1)}{a_R^2} + \frac{2l(l+1)}{a_R^3} \xi_2 \right) \tilde{R}_{l_2}(r) = 0 \quad (36)$$

Changing variables once again using

$$x_2 = \left(\frac{2l(l+1)}{a_R^3} \right)^{1/3} \xi_2 \quad (37)$$

Eq.(36) assumes the simple canonical form

$$\frac{d^2 \tilde{R}_{l_2}}{dx_2^2} - t \tilde{R}_{l_2} = 0 \quad (38)$$

where

$$t \equiv (t_2(l) - x_2) \quad (39)$$

and

$$t_2(l) \equiv - \left(\frac{a_R^3}{2l(l+1)} \right)^{2/3} \left(k_2^2 - \frac{l(l+1)}{a_R^2} \right) \quad (40)$$

The solutions to the differential equation of Eq.(38) are in terms of the Airy function which will be discussed much more completely in the next section.

The parameter $t_2(l)$ determines the modes of the radial function given by Eq.(38). To examine the relationship between this quantity and that of the product $l(l+1)$, one can write Eq.(39) in the following form

$$(L - \Lambda)^3 = 2^2 t_2^3(l) L^2 \quad (41)$$

where

$$L \equiv l(l+1), \quad \Lambda \equiv k_2^2 a_R^2 \quad (42)$$

Solving the cubic equation that results from the expansion of Eq.(41) and selecting the real solution out of the three roots that correspond to the total solution gives a relationship that involves many terms. However, in the event that one has $t_2(l) \ll \Lambda^{1/3}$, the solution can be expanded to give

$$\begin{aligned} L &= \Lambda \left[1 + 2^{1/3} \frac{t_2}{\Lambda^{1/3}} \left\{ 2 + \frac{144}{54\Lambda} t_2^3 + \dots \right\}^{1/3} + \frac{8}{3(2^{2/3})\Lambda^{2/3}} \frac{t_2^2}{\Lambda^{2/3}} + \dots \right] \\ &= \Lambda \left[1 + 2^{2/3} \frac{t_2}{\Lambda^{1/3}} + \frac{4}{3} 2^{1/3} \frac{t_2^2}{\Lambda^{2/3}} + \dots \right] \\ &\approx (k_2 a_R)^2 \left[1 + \left(\frac{2}{k_2 a_R} \right)^{2/3} t_2 \right], \quad t_2(l) \ll (k_2 a_R)^{2/3} \end{aligned} \quad (43)$$

This is a most important result that will be employed many times throughout this work; the combination $l(l+1)$ can be approximately replaced by $(ka)^2$ in which the k or a values are peculiar to the region being considered. In some other cases, as will be indicated, the entire expression of Eq.(43) will be used. In fact, one can return to Eq.(31) and use this result to obtain for the surface impedance at $r = a - \delta = a_R$

$$Z_1 = - \frac{1}{\epsilon_1^{1/2}} \left(1 - \frac{k_2^2}{k_1^2} \right)^{1/2} \quad (44)$$

Although Eq.(40) is the formal solution for the radial component of the potential within the regolith, one can obtain a simpler, approximate solution which exploits the thin layer that defines the regolith. Returning to Eq.(36) and using the fact that $a_R \approx a$ (i.e., $\delta \ll a$) and $\xi_2 \ll a$, one can write

$$\frac{d^2 \tilde{R}_{l_2}(r)}{d\xi_2^2} + \left(k_2^2 - \frac{l(l+1)}{a^2} \right) \tilde{R}_{l_2}(r) = 0 \quad (45)$$

the solution of which is simply

$$\tilde{R}_{l_2}(r) = A_2 e^{+i\kappa_{l_2}(r-a_R)} + B_2 e^{-i\kappa_{l_2}(r-a_R)}, \quad a_R < r < a \quad (46)$$

where

$$\kappa_{l_2} \equiv \left(k_2^2 - \frac{l(l+1)}{a^2} \right)^{1/2} \quad (47)$$

As before, the determination of the values for $l(l+1)$ is connected to the radial equation which prevails in region 3, the exosphere. Substituting Eq.(46) into Eq.(13) yields for the scalar potential in this region

$$U_{e_2}(r, \theta) = \frac{A_2 e^{+i\kappa_{l_2}(r-a_R)} + B_2 e^{-i\kappa_{l_2}(r-a_R)}}{r} P_l(-\cos \theta) \quad (48)$$

Once again, from Eqs.(10) and (11), the corresponding fields are

$$E_{\theta_2}(r, \theta) = \frac{A_2 (+i\kappa_{l_2}) e^{+i\kappa_{l_2}(r-a_R)} + B_2 (-i\kappa_{l_2}) e^{-i\kappa_{l_2}(r-a_R)}}{r} \frac{\partial P_l(-\cos \theta)}{\partial \theta} \quad (49)$$

$$H_{\phi_2}(r, \theta) = +ik_0 n_2^2 \frac{A_2 e^{+i\kappa_{l_2}(r-a_R)} + B_2 e^{-i\kappa_{l_2}(r-a_R)}}{r} \frac{\partial P_l(-\cos \theta)}{\partial \theta} \quad (50)$$

These components must be matched to the previously calculated surface impedance at $r = a_R$. To this end, the surface impedance within region 2 at the surface $r = a_R$ is defined by

$$Z_2 \equiv - \frac{E_{\theta_2}(r, \theta)}{H_{\phi_2}(r, \theta)} \Big|_{r=a_R} \quad (51)$$

Hence, using Eqs.(49) and (50), one obtains, after simplification,

$$Z_2 = -\frac{\kappa_{l_2}(A_2 - B_2)}{k_0 \varepsilon_2 (A_2 + B_2)} \quad (52)$$

Since $Z_1 = Z_2$, equating Eqs.(44) and (52) gives

$$\frac{A_2 - B_2}{A_2 + B_2} = \frac{k_2}{\kappa_{l_2}} \Delta_{12} \quad (53)$$

where

$$\Delta_{12} \equiv \left(\frac{\varepsilon_2}{\varepsilon_1} \right)^{1/2} \left(1 - \frac{k_2^2}{k_1^2} \right)^{1/2} \quad (54)$$

From Eq.(53), one obtains the amplitude ratio

$$\frac{B_2}{A_2} = \frac{\kappa_{l_2} - k_2 \Delta_{12}}{\kappa_{l_2} + k_2 \Delta_{12}} \quad (55)$$

d. Solution for Region 3 in the Special Case of No Exospheric Plasma

At the outset of deriving the full solution for the charged exosphere, the simplified case where $\varepsilon_3(\xi_3) = 1$ in region 3 will be considered first. That is, only the effects of diffraction and the presence of the regolith will be considered here. This will allow establishing of several mathematical techniques, especially those having to do with interfacing the source conditions into the solution, which will prove useful in the more complicated case in which $\varepsilon_3(\xi_3)$ is given by Eq.(7). Equation (17) becomes, in this case,

$$\frac{d^2 \tilde{R}_{l_3}(r)}{dr^2} + \left(k_3^2 - \frac{l(l+1)}{r^2} \right) \tilde{R}_{l_3}(r) = 0, \quad k_3^2 = k_0^2, \quad a \leq r, \quad \xi_3 = r - a \quad (56)$$

As before, one can adopt the approximation

$$r^{-2} = (a + \xi_3)^{-2} = a^{-2} \left(1 + \frac{\xi_3}{a} \right)^{-2} \approx a^{-2} \left(1 - 2 \frac{\xi_3}{a} \right) \quad (57)$$

allowing Eq.(56) to become

$$\frac{d^2 \tilde{R}_{l_3}(r)}{dr^2} + \left(k_3^2 - \frac{l(l+1)}{a^2} + 2 \frac{l(l+1)}{a^3} \xi_3 \right) \tilde{R}_{l_3}(r) = 0 \quad (58)$$

This is the same form as Eq.(36); thus, following the same procedure as earlier, one can write

$$\frac{d^2 \tilde{R}_{l_3}}{dx_3^2} - t \tilde{R}_{l_3} = 0 \quad (59)$$

where

$$t \equiv (t_3(l) - x_3) \quad (60)$$

with

$$t_3(l) \equiv - \left(\frac{a^3}{2l(l+1)} \right)^{2/3} \left(k_3^2 - \frac{l(l+1)}{a^2} \right) \quad (61)$$

Here,

$$x_3 = \left(\frac{2l(l+1)}{a^3} \right)^{1/3} \xi_3 \quad (62)$$

A solution to the differential equation of Eq.(59) is in terms of the Airy function $w_1(t)$ or $Ai(x)$ [11,12,13]

$$\tilde{R}_{l_3}(x_3) = A_2 w_1(t) = A_2 2\sqrt{\pi} e^{i\frac{\pi}{6}} Ai\left(te^{i\frac{2\pi}{3}} \right) \quad (63)$$

where $w_1(t)$ is the Airy function as defined by Fock [12] and $Ai(\dots)$ is the Airy function as originally defined by Miller [14]; the latter function is used in most mathematical references [13]. (There is a second solution to Eq.(59) denoted by $w_2(t)$ or $Bi(\dots)$ but is ignored here due to violation of boundary conditions at $t \rightarrow \infty$.)

As before, following the procedure leading to Eq.(43) with $t_3(l) \ll (k_3 a)^{2/3}$ prevailing, one has

$$l(l+1) \approx (k_3 a)^2 \left[1 + \left(\frac{2}{k_3 a} \right)^{2/3} t_3 \right] \approx (k_3 a)^2 \quad (64)$$

Hence, using Eq.(47), Eq.(55) becomes

$$\frac{B_2}{A_2} = \frac{(k_2^2 - k_3^2)^{1/2} - k_2 \Delta_{12}}{(k_2^2 - k_3^2)^{1/2} + k_2 \Delta_{12}} \quad (65)$$

Now, using the general solution given by Eq.(13), one has for the scalar electric potential in region 3

$$U_{e_3}(r, \theta) = A_3 \frac{w_1(t_3 - x_3)}{r} P_l(-\cos \theta) \quad (66)$$

where A_3 is another constant. But, by Eqs.(62) and (64),

$$\begin{aligned} x_3 &= \left(\frac{2k_3^2}{a} \right)^{1/3} (r - a) \\ &= \beta(r - a), \quad \beta \equiv k_3 \left(\frac{2}{k_3 a} \right)^{1/3} \end{aligned} \quad (67)$$

Hence, Eq.(66) becomes

$$U_{e_3}(r, \theta) = A_3 \frac{w_1(t_3 - \beta(r - a))}{r} P_l(-\cos \theta) \quad (68)$$

which, when used in Eqs.(10) and (11) applied to region 3 gives, respectively,

$$E_{\theta_3}(r, \theta) = -\beta \left(\frac{A_3}{r} \right) w_1'(t_3 - \beta(r - a)) \frac{\partial P_l(-\cos \theta)}{\partial \theta} \quad (69)$$

and

$$H_{\phi_3}(r, \theta) = +ik_0 n_3^2 \left(\frac{A_3}{r} \right) w_1(t_3 - \beta(r - a)) \frac{\partial P_l(-\cos \theta)}{\partial \theta} \quad (70)$$

Rather than defining two more impedances across the surface $r = a$ and equating, one can match the electric and magnetic fields across this boundary straightaway. Thus, equating Eqs.(49) and (69) at $r = a$ gives

$$-A_3 \beta w_1'(t_3) = A_2 (i\kappa_{l_2}) \left[e^{i\kappa_{l_2} \delta} - \frac{B_2}{A_2} e^{-i\kappa_{l_2} \delta} \right] \quad (71)$$

Similarily, equating Eqs.(50) and (70) at this boundary yields

$$n_3^2 A_3 w_1(t_3) = A_2 n_2^2 \left[e^{i\kappa_{l_2} \delta} + \frac{B_2}{A_2} e^{-i\kappa_{l_2} \delta} \right] \quad (72)$$

Finally, taking the ratio of these two results gives the transcendental equation for t_3

$$w_1'(t_3) - q w_1(t_3) = 0 \quad (73)$$

where

$$q = -i \left(\frac{1}{\varepsilon_2} \right) \left(\frac{1}{k_0} \right) \left(\frac{k_0 a}{2} \right)^{1/3} \kappa_{l_2} \left[\frac{e^{i\kappa_{l_2} \delta} - \frac{B_2}{A_2} e^{-i\kappa_{l_2} \delta}}{e^{i\kappa_{l_2} \delta} + \frac{B_2}{A_2} e^{-i\kappa_{l_2} \delta}} \right], \quad \kappa_{l_2} \equiv (k_2^2 - k_3^2)^{1/2} = (k_2^2 - k_0^2)^{1/2} \quad (74)$$

Given all the parameters that define the propagation problem, one determines, with the help of Eq.(55), the prevailing value for q . The solution to Eq.(73) gives a spectrum of values for the quantity t_3 which determines the propagation modes of the electromagnetic radiation that can exist in region 3. It remains now to introduce a source of the radiation and couple it to the expression for the scalar potential, Eq.(68).

To this end, return to Eq.(63) and normalize the solution at the boundary $r = a$. Thus, defining

$$\tilde{R}_3(x_3) \Big|_{r=a} = A_3 w_1(t_3) = 1 \quad (75)$$

determines the constant A_3 . Using this result in Eq.(68) and remembering that there are many values t_{3_j} , $j = 1, 2, \dots$, for t_3 that issue from Eq.(73), one can rewrite Eq.(68) by employing superposition and obtain

$$U_{e_3}(r, \theta) = \sum_{j=1}^{\infty} A_j \frac{w_1(t_{3_j} - x_3)}{w_1(t_{3_j})} \left(\frac{1}{r} \right) P_l(-\cos \theta) \quad (76)$$

where A_j is an array of constants, one for each mode, to be determined by the source boundary conditions. These constants are defined to be the modal amplitudes, i.e., the amplitude of each of the modes supported along the lunar surface.

i. Derivation of the Equation for the Modal Amplitudes

In an effort to isolate the A_j factors, one can attempt to treat the quotients $w_1(t_{3_j} - x_3) / w_1(t_{3_j'})$ as a set of orthogonal functions; this could be possible since the Airy functions come from a second-order differential equation. Therefore, consider the following development

$$\int_0^{\infty} r U_{e_3}(r, \theta) \frac{w_1(t_{3_j'} - x_3)}{w_1(t_{3_j'})} d\xi_3 \frac{1}{P_l(-\cos \theta)} = \sum_{j=1}^{\infty} \int_0^{\infty} A_j \frac{w_1(t_{3_j'} - x_3)}{w_1(t_{3_j'})} \frac{w_1(t_{3_j} - x_3)}{w_1(t_{3_j})} d\xi_3 \quad (77)$$

remembering that $x_3 = \beta \xi_3$, $\xi_3 = r - a$. The integral occurring on the right side of Eq.(77) will now be reduced using all the known properties of the functions $w_1(\dots)$. These properties are, from Eqs.(59), (60), and (73)

$$\frac{d^2 w_1(t_{3_j} - x_3)}{dx_3^2} - (t_{3_j} - x_3) w_1(t_{3_j} - x_3) = 0 \quad (78)$$

and

$$\frac{dw_1(t_{3_j} - x_3)}{dx_3} - q w_1(t_{3_j} - x_3) = 0 \quad (79)$$

The first relation is the definition of $w_1(\dots)$ and the second is the associated boundary condition. Multiplying Eq.(78) by the function $w_1(t_{3_j'} - x_3)$ and, conversely, multiplying Eq.(78) applied at $t_{3_j'}$ by $w_1(t_{3_j} - x_3)$ and subtracting the latter from the former gives

$$\begin{aligned} w_1(t_{3_j'} - x_3) \frac{d^2 w_1(t_{3_j} - x_3)}{dx_3^2} - w_1(t_{3_j} - x_3) \frac{d^2 w_1(t_{3_j'} - x_3)}{dx_3^2} &= \\ &= (t_{3_j} - t_{3_j'}) w_1(t_{3_j} - x_3) w_1(t_{3_j'} - x_3) \end{aligned} \quad (80)$$

Letting $x_3 \equiv \beta z$ and integrating Eq.(80) with respect to z yields, after integrating by parts,

$$\frac{1}{\beta} \left[w_1(t_{3_j'} - x_3) \frac{dw_1(t_{3_j} - x_3)}{dx_3} - w_1(t_{3_j} - x_3) \frac{dw_1(t_{3_j'} - x_3)}{dx_3} \right] \Bigg|_0^{\infty} =$$

$$= \left(t_{3_j} - t_{3_{j'}} \right) \int_0^\infty w_1 \left(t_{3_j} - \beta z_3 \right) w_1 \left(t_{3_{j'}} - \beta z_3 \right) dz_3 \quad (81)$$

Hence, by Eq.(79), one has

$$\int_0^\infty w_1 \left(t_{3_j} - \beta z_3 \right) w_1 \left(t_{3_{j'}} - \beta z_3 \right) dz_3 = 0, \quad t_{3_j} \neq t_{3_{j'}} \quad (82)$$

Thus, the Airy functions as defined by this problem are orthogonal. For the case in which $t_{3_j} = t_{3_{j'}}$, one must return to Eq.(81) and consider

$$\begin{aligned} \lim_{t_{3_j} \rightarrow t_{3_{j'}}} \int_0^\infty w_1 \left(t_{3_j} - \beta z_3 \right) w_1 \left(t_{3_{j'}} - \beta z_3 \right) dz_3 &= \\ &= \int_0^\infty w_1^2 \left(t_{3_j} - \beta z_3 \right) \\ &= \lim_{t_{3_j} \rightarrow t_{3_{j'}}} \frac{\left[w_1 \left(t_{3_j} - x_3 \right) \frac{dw_1 \left(t_{3_j} - x_3 \right)}{dx_3} - w_1 \left(t_{3_j} - x_3 \right) \frac{dw_1 \left(t_{3_j} - x_3 \right)}{dx_3} \right]_0^\infty}{\beta \left(t_{3_j} - t_{3_{j'}} \right)} \end{aligned} \quad (83)$$

Employing L'Hospital's rule and differentiating both the numerator and denominator by t_{3_j} gives

$$\begin{aligned} \int_0^\infty w_1^2 \left(t_{3_j} - \beta z_3 \right) &= \frac{1}{\beta} \left[w_1 \left(t_{3_j} - x_3 \right) \frac{d^2 w_1 \left(t_{3_j} - x_3 \right)}{dt_{3_j} dx_3} - \frac{dw_1 \left(t_{3_j} - x_3 \right)}{dt_{3_j}} \frac{dw_1 \left(t_{3_j} - x_3 \right)}{dx_3} \right]_0^\infty \\ &= \frac{1}{\beta} \left[-w_1 \left(t_{3_j} - x_3 \right) \frac{d^2 w_1 \left(t_{3_j} - x_3 \right)}{dx_3^2} + \frac{dw_1 \left(t_{3_j} - x_3 \right)}{dx_3} \frac{dw_1 \left(t_{3_j} - x_3 \right)}{dx_3} \right]_0^\infty \end{aligned} \quad (84)$$

Finally, using Eqs.(78) and (79), Eq.(84) reduces to

$$\int_0^\infty w_1^2 \left(t_{3_j} - \beta z_3 \right) = \frac{1}{\beta} \left(t_{3_j} - q^2 \right) w_1^2 \left(t_{3_j} \right) \quad (85)$$

upon noting the fact that the term at infinity vanishes due to the asymptotic properties of the $w_1(\dots)$ functions. Hence, returning to the original expression on the left side of Eq.(77), one has from Eqs.(82) and (85),

$$\sum_{j=1}^{\infty} \int_0^{\infty} A_j \frac{w_1(t_{3_j} - x_3) w_1(t_{3_j} - x_3)}{w_1(t_{3_j}) w_1(t_{3_j})} d\xi_3 = A_{j'} \frac{1}{\beta} (t_{3_j} - q^2) \quad (86)$$

thus isolating the modal amplitude $A_{j'}$, viz, using Eq.(86) in Eq.(77) gives

$$A_j = \frac{\beta}{(t_{3_j} - q^2) P_1(-\cos \theta)} \int_0^{\infty} r U_{e_3}(r, \theta) \frac{w_1(t_{3_j} - x_3)}{w_1(t_{3_j})} d\xi_3 \quad (87)$$

ii. Evaluation Of the Modal Amplitudes for a Given Source Distribution

The evaluation of the expression of Eq.(87) must be done by specifying the source of the electromagnetic radiation in terms of its electric scalar potential. Using a technique that dates back to Sommerfeld [15] which is briefly detailed by Wait [16], let the source of radiation be a vertical electric dipole of length L be placed at $\theta = 0$ and subtending an interval $\xi_{3_s} \leq \xi_3 \leq \xi_{3_s} + L$ along the radial coordinate. The integral in Eq.(87) must now be evaluated in the immediate neighborhood of this source. The electric scalar potential for an electrically small dipole source is, reckoned to the radial coordinate [17],

$$r_s U_{e_{30}}(r, \theta) = i \frac{JL}{\omega} \frac{e^{ik_3 D}}{D}, \quad D \equiv (r_s^2 + r^2 - 2r_s r \cos \theta)^{1/2} \quad (88)$$

where $r_s = a + \xi_{3_s}$, J is the current density within the dipole, ω is the angular frequency of the radiation ($\omega = k_3 c$), and D is the distance to the dipole from the location r . The angle θ is the angular displacement between the two radii r_s and r . In the evaluation of the integral of Eq.(87), the point $r \rightarrow r_s$ thus requiring the limit $\theta \rightarrow 0$. With these provisos, substituting Eq.(88) into Eq. (87) gives

$$\int_0^{\infty} r U_{e_3}(r, \theta) \frac{w_1(t_{3_j} - x_3)}{w_1(t_{3_j})} d\xi_3 = \lim_{\theta \rightarrow 0} i \left(\frac{JL}{\omega} \right) \int_a^{\infty} \left(\frac{r}{r_s} \right) \frac{w_1(t_{3_j} - \beta(r - a))}{w_1(t_{3_j})} \frac{e^{ik_3 D}}{D} dr \quad (89)$$

Since r_s is taken to be the distance to the center of the dipole of total length L , the length the dipole subtends along the radial coordinate can be written as

$$r = r_s (1 + \eta), \quad \frac{-L/2}{r_s} \leq \eta \leq \frac{L/2}{r_s} \quad (90)$$

Equation (89) can then be written as

$$\int_0^{\infty} r U_{e_3}(r, \theta) \frac{w_1(t_{3_j} - x_3)}{w_1(t_{3_j})} d\xi_3 = \lim_{\theta \rightarrow 0} i \left(\frac{JL}{\omega} \right) \int_{-L/2}^{L/2} \frac{r_s}{r_s} (1 + \eta) \frac{w_1(t_{3_j} - \beta(r_s(1 + \eta) - a))}{w_1(t_{3_j})} \frac{e^{ik_3 D}}{D} r_s d\eta$$

$$\approx i \left(\frac{JL}{\omega} \right) \frac{w_1(t_{3_j} - \beta(r_s - a))}{w_1(t_{3_j})} \lim_{\theta \rightarrow 0} \int_{-L/2}^{L/2} \frac{e^{ik_3 r_s (\eta^2 + \theta^2)^{1/2}}}{(\eta^2 + \theta^2)^{1/2}} d\eta \quad (91)$$

where the second result issues from the fact that $(L/2)/r_s \ll 1$ and $\cos \theta \approx \theta$ for $\theta \rightarrow 0$. Since the dipole is taken to be electrically small, i.e., $L \ll \lambda$, the exponential within the integral of Eq.(91) can be taken to be equal to unity. In this case, the remaining integral can be performed to give

$$\int_0^{\infty} r U_{e_3}(r, \theta) \frac{w_1(t_{3_j} - x_3)}{w_1(t_{3_j})} d\xi_3 \approx i \left(\frac{JL}{\omega} \right) \frac{w_1(t_{3_j} - \beta(r_s - a))}{w_1(t_{3_j})} \lim_{\theta \rightarrow 0} \ln \left[\frac{\left(\left(\frac{L/2}{r_s} \right)^2 + \theta^2 \right)^{1/2} + \frac{L/2}{r_s}}{\left(\left(\frac{L/2}{r_s} \right)^2 + \theta^2 \right)^{1/2} - \frac{L/2}{r_s}} \right]$$

$$= i \left(\frac{JL}{\omega} \right) \frac{w_1(t_{3_j} - \beta(r_s - a))}{w_1(t_{3_j})} (-\ln \theta^2), \quad \theta \rightarrow 0 \quad (92)$$

where the last result is obtained by asymptotically evaluating the limit of the logarithm. Therefore, Eq.(87) becomes

$$A_j = \frac{\beta}{(t_{3_j} - q^2) P_l(-\cos \theta)} i \left(\frac{JL}{\omega} \right) \frac{w_1(t_{3_j} - \beta(r_s - a))}{w_1(t_{3_j})} (-\ln \theta^2), \quad \theta \rightarrow 0 \quad (93)$$

However, the condition $\theta \rightarrow 0$ is prevailing for this expression; hence, the Legendre polynomial in the denominator must be evaluated in this limit. Using the well-known [18] asymptotic form

$$\lim_{\theta \rightarrow 0} P_l(-\cos \theta) = \frac{\sin l\pi}{\pi} \ln \left(\frac{1 - \cos \theta}{2} \right) \approx \frac{\sin l\pi}{\pi} \ln \theta^2 \quad (94)$$

the expression for the modal amplitude finally becomes

$$A_j = - \frac{\pi \beta}{(t_{3_j} - q^2) \sin l\pi} i \left(\frac{JL}{\omega} \right) \frac{w_1(t_{3_j} - \beta(r_s - a))}{w_1(t_{3_j})} \quad (95)$$

iii. The Electric Scalar Potential and Associated Radial Electric Field

Returning to Eq.(76) for the electric scalar potential in region 3 and substituting into it Eq.(95) gives

$$U_{e_3}(r, \theta) = -\frac{\pi\beta}{\sin l\pi} i \left(\frac{JL}{\omega} \right) \sum_{j=1}^{\infty} \frac{1}{(t_{3_j} - q^2)} \frac{w_1(t_{3_j} - \beta(r_s - a))}{w_1(t_{3_j})} \cdot \frac{w_1(t_{3_j} - \beta(r - a))}{w_1(t_{3_j})} \left(\frac{1}{r} \right) P_l(-\cos \theta) \quad (96)$$

At this point, another approximation is in order. From Eq.(64), one has

$$l \approx (k_3 a) \left[1 + \left(\frac{2}{k_3 a} \right)^{2/3} t_{3_j} \right]^{1/2} \approx k_3 a + \left(\frac{k_3 a}{2} \right)^{1/3} t_{3_j} \quad (97)$$

Thus, the value for l is such that $l \gg 1$. In addition, the roots of Eq.(73) will be complex and thus, in general, l will possess a large complex part. One can then employ another asymptotic expansion of the Legendre function for large orders [19], viz,

$$\lim_{|l| \rightarrow \infty} P_l(-\cos \theta) = P_l(\cos(\pi - \theta)) = \left(\frac{2}{\pi l \sin \theta} \right)^{1/2} \sin \left[\left(l + \frac{1}{2} \right) (\pi - \theta) + \frac{\pi}{4} \right] \quad (98)$$

The use of this expansion in Eq.(96) results in a rather unwieldy expression which would be difficult to treat. At this point, the following method is adopted [20]. From the identity $\sin \varphi = (e^{i\varphi} - e^{-i\varphi})/2i$, one has that if $\text{Im} \{\varphi\} \gg 1$, the first exponential will decay away giving $\sin \varphi = -e^{-i\varphi}/2i$. Hence, since $\text{Im} \{l\} \gg 1$ as per Eq.(97), Eq.(98) can be written

$$\lim_{|l| \rightarrow \infty} P_l(-\cos \theta) = -\left(\frac{2}{\pi l \sin \theta} \right)^{1/2} \left(\frac{1}{2i} \right) e^{-i[(l+1/2)(\pi-\theta)+\pi/4]} \quad (99)$$

Similarly,

$$\sin l\pi = \frac{-e^{-il\pi}}{2i} \quad (100)$$

Using Eqs.(97), (99), and (100) in Eq.(96) yields, after simplification,

$$U_{e_3}(r, \theta) = -2\pi i \beta \left(\frac{JL}{\omega} \right) \left(\frac{1}{2\pi k_3 a \sin \theta} \right)^{1/2} e^{-i3\pi/4} e^{ik_3 a \theta} \cdot \left(\frac{1}{r} \right) \sum_{j=1}^{\infty} \left(\frac{1}{t_{3_j} - q^2} \right) \frac{w_1(t_{3_j} - \beta(r_s - a)) w_1(t_{3_j} - \beta(r - a))}{w_1(t_{3_j}) w_1(t_{3_j})} e^{ix(\theta)t_{3_j}} \quad (101)$$

where $x(\theta) \equiv \theta(k_3 a/2)^{1/3}$ is the scaled angular displacement from the source, sometimes called the reduced horizontal distance from the source [21].

With the electric scalar potential in hand, one can now obtain expressions for any component of the electromagnetic field along the lunar surface. What is of interest here, however, is the electric field component existing along the radial direction; this is given by Eq.(A40) of Appendix A, viz,

$$E_{r_3}(r, \theta) = -\frac{1}{r \sin \theta} \frac{\partial}{\partial \theta} \left(\sin \theta \frac{\partial U_{e_3}}{\partial \theta} \right) \quad (102)$$

But, by Eqs.(B18) and (B26), one has

$$\frac{1}{\sin \theta} \frac{\partial}{\partial \theta} \left(\sin \theta \frac{\partial U_{e_3}}{\partial \theta} \right) + l(l+1)U_{e_3} = 0 \quad (103)$$

Therefore,

$$E_{r_3}(r, \theta) = \frac{l(l+1)}{r} U_{e_3}(r, \theta) = \frac{(k_3 a)^2}{r} U_{e_3}(r, \theta) \quad (104)$$

Hence, for the radial electric field in region 3 above the lunar surface with no exosphere, one has

$$E_{r_3}(r, \theta) = -2i\pi e^{-i3\pi/4} (k_3 a)^2 \beta \left(\frac{1}{r^2} \right) \left(\frac{JL}{\omega} \right) \left(\frac{1}{2\pi k_3 a \sin \theta} \right)^{1/2} e^{ik_3 a \theta} \cdot \sum_{j=1}^{\infty} \left(\frac{1}{t_{3_j} - q^2} \right) \frac{w_1(t_{3_j} - \beta(r_s - a)) w_1(t_{3_j} - \beta(r - a))}{w_1(t_{3_j}) w_1(t_{3_j})} e^{ix(\theta)t_{3_j}} \quad (105)$$

Finally, letting the height to the source from the lunar surface be $\xi_{3_s} = r_s - a$ and similarly the height from the surface to the receiving point be $\xi_{3_r} = r - a$ and noting that $r^{-2} = (\xi_{3_r} + a)^{-2} \approx a^{-2}$, one has, upon using the definition for β and rearranging factors

$$E_{t_3}(\xi_{3_r}, \theta) = E_0(\theta) V(x(\theta), \xi_{3_s}, \xi_{3_r}, q) \quad (106)$$

where

$$V(x(\theta), \xi_{3_s}, \xi_{3_r}, q) \equiv 2e^{i\pi/4} (\pi x(\theta))^{1/2} \sum_{j=1}^{\infty} \left(\frac{1}{t_{3_j} - q^2} \right) \frac{w_1(t_{3_j} - \beta \xi_{3_s})}{w_1(t_{3_j})} \frac{w_1(t_{3_j} - \beta \xi_{3_r})}{w_1(t_{3_j})} e^{ix(\theta)t_{3_j}} \quad (107)$$

is the ‘attenuation factor’ [22] and

$$E_0(\theta) \equiv ik_3^2 \left(\frac{JL}{\omega} \right) \frac{e^{ik_3 a \theta}}{a(\theta \sin \theta)^{1/2}} \quad (108)$$

is the non-diffracted electric field strength. Equation (107) is the celebrated expression, originally obtained using other methods by Fock [23], for the diffracted electric field strength of an electromagnetic field along the surface of, in this case, the moon. The effect of the regolith is convolved in the parameter q given by Eq.(74) as well as in the solutions t_{3_j} of the modal equation, Eq.(73). It remains now to solve Eq.(73) for the spectrum of t_{3_j} values and incorporate them into Eq.(107) for evaluation.

iv. Numerical Evaluation of the Modal Equation and of the Electric Field

One must necessarily commence with the numerical evaluation of Eq.(73) in order to obtain the array of t_{3_j} values to be used in Eq.(107). It is useful to decompose these values into their real and imaginary parts, viz.,

$$t_{3_j} = x_j + iy_j \quad (108)$$

Since the evaluation of these expressions will be done using *Mathematica*, and *Mathematica* only uses the Airy functions $Ai(\dots)$ as well as its derivative $Ai'(\dots)$, one must use the representation given in Eq.(63) and rewrite Eq.(73) as

$$e^{i\frac{2\pi}{3}} Ai' \left((x_j + iy_j) e^{i\frac{2\pi}{3}} \right) - q Ai \left((x_j + iy_j) e^{i\frac{2\pi}{3}} \right) = 0 \quad (109)$$

By plotting zeros of the real and imaginary parts of this expression with respect to x_j and y_j , one can immediately identify its roots to be at the points where the zero contours intersect one another.

For example, take the frequency of operation to be 100 KHz; the relevant electrical properties are taken as displayed in Table.1. Using these values in Eqs.(54),

(65) and (74) (noting that $k_3 = k_0$ here since $\varepsilon_1 = 1$ as the exosphere is absent), one obtains that in the case of no regolith ($\delta = 0$)

$$q = -0.857 - 0.936i \quad (110)$$

Using this value in Eq.(109) and plotting the zeros of the real and imaginary parts of this expression gives the plot displayed in Figure 5.

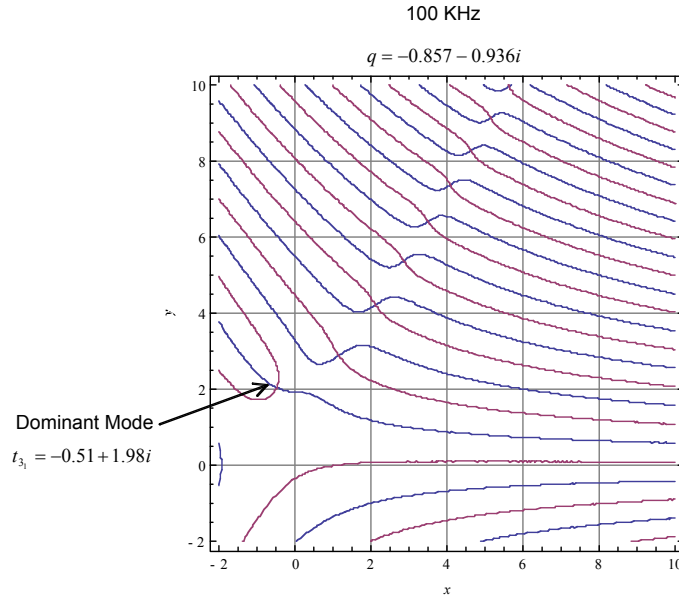


Figure 5. Real (x) and Imaginary (y) Parts of the Argument of Eq.(109).

Here, eight modal values of t_{3_j} are displayed. The first root t_{3_1} is the dominant mode since it has the smallest imaginary part and will thus yield the smallest attenuation occurring in the $e^{ix(\theta)t_{3_1}}$ factor of Eq.(106). Due to this attenuation contributed by $\text{Im} \{t_{3_j}\} > 0$, only the first four or five values of t_{3_j} need be used in the evaluation of Eq.(107) as the $e^{ix(\theta)t_{3_1}}$ factor will quickly decay away for large $\text{Im} \{t_{3_j}\}$. All other calculations similarly follow. In some cases, one will encounter the first root in which $\text{Im} \{t_{3_1}\} < 0$ is an unphysical result and is thus an extraneous root. Hence, the root must be rejected and the next root above it for which $\text{Im} \{t_{3_j}\} > 0$ becomes the root corresponding to the dominant mode.

In the results that are to follow, transmitter and receiver antennas are, respectively, 20 m and 2 m above the lunar surface ($\xi_{3_s} = 2000$ cm, $\xi_{3_r} = 200$ cm), and the transmitter is taken to have a power output of 1 W. The transmitting dipole length is 10 m. Cases for the transmitting frequency of 50 KHz, 100 KHz, 200 KHz, 500 KHz and 1 MHz are shown in Figures 6-10 which show electric field strength in volts/meter versus

distance from the source in kilometers. At 50 KHz, there does not appear a trapped surface wave phenomenon; each case is not too different from the others. Figure 7 displays the rather interesting situation at 100 KHz in which the $\delta = 100$ m case does much worse than that where $\delta = 0$; here, the electric field intensity is almost an order of magnitude down from that of $\delta = 0$ at a distance of 100 Km. The regolith of $\delta = 100$ m attenuates the wave along the surface as compared to the other cases. However, for $\delta = 50$ m, a trapped wave phenomenon seems to occur allowing the field strength to be more than an order of magnitude greater than for the $\delta = 0$ case.

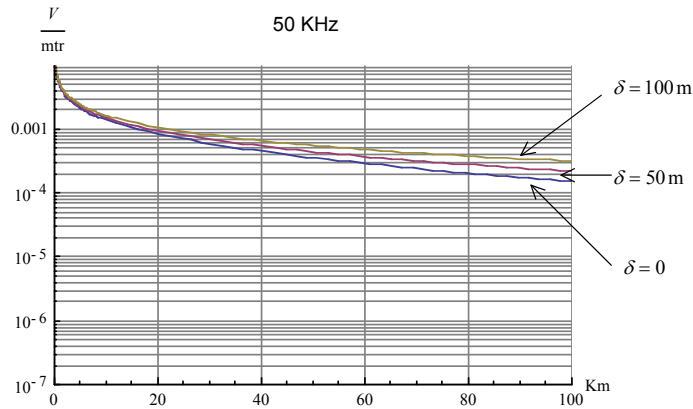


Figure 6. Electric Field Strength vs. Distance Along Lunar Surface at 50 KHz

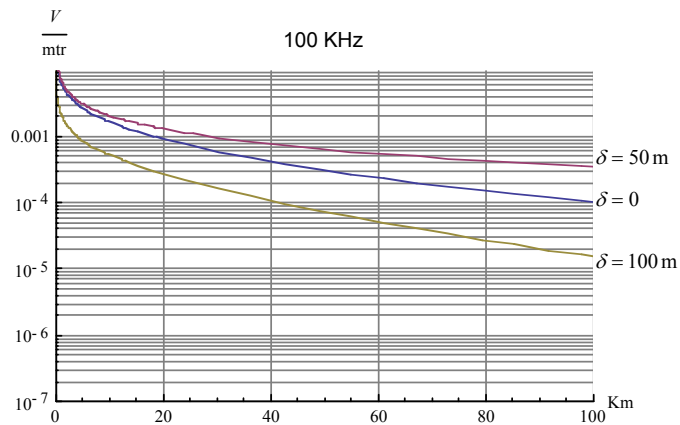


Figure 7. Electric Field Strength vs. Distance Along Lunar Surface at 100 KHz

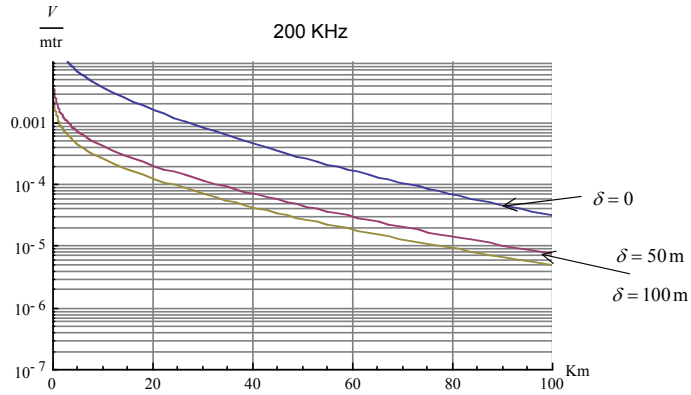


Figure 8. Electric Field Strength vs. Distance Along Lunar Surface at 200 KHz

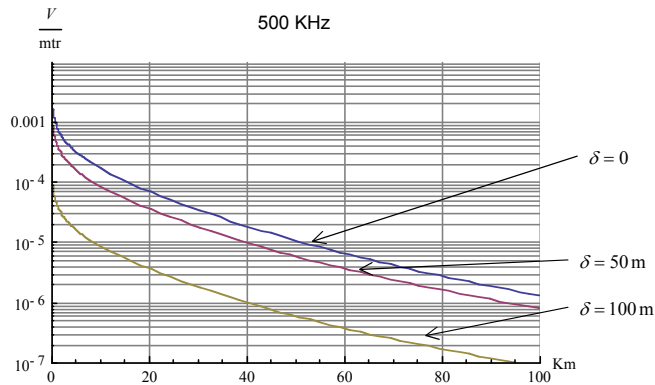


Figure 9. Electric Field Strength vs. Distance Along Lunar Surface at 500 KHz

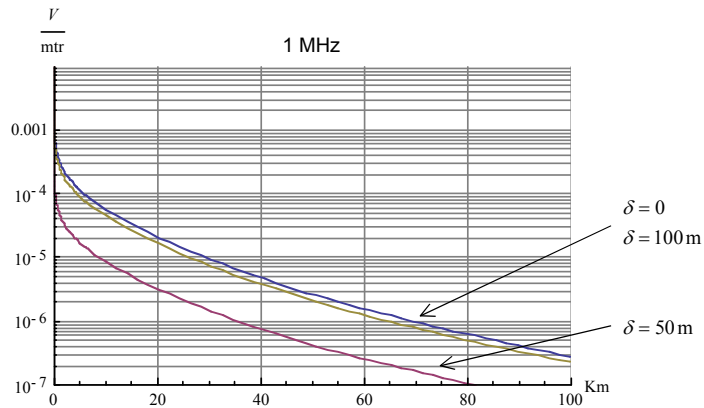


Figure 10. Electric Field Strength vs. Distance Along Lunar Surface at 1 MHz

At 200 KHz as shown in Fig. 8, the trapped surface wave ceases to exist and both regolith cases do worse than that for $\delta = 0$. From this example on, the regolith attenuates the propagating wave field along the surface as shown in Figs. 9 and 10. Hence, the use

of frequencies below 100 KHz would not be warranted in order to exploit the trapped surface, ‘whispering gallery’ wave phenomenon. However, what is most disconcerting is the fact that in the real case of the lunar regolith, one cannot expect it to remain at a given depth. In fact, the regolith depth will be some highly random function of direction and distance from the transmitter site. Hence, one can expect that, given the enhancement and attenuation of the varying regolith thickness, the electric field strength will most likely be approximately at the value realized with the case $\delta = 0$ at 100 KHz. This, of course, requires a more detailed investigation.

The behavior of the signal field strength as a function of both frequency and regolith depth also requires a more careful investigation than given here. The analysis of this spherical dielectric waveguide problem would not be too different than that used to study the cavity formed by the Earth and ionosphere [24].

e. Solution for Region 3 for the Case of an Exospheric Plasma

The solution of the general problem defined by Eq.(17) using the permittivity profile given by Eq.(7) will now be addressed using the mathematical methodology established in Section III.d. Thus, one must now deal with the differential equation

$$\frac{d^2 \tilde{R}_{l_3}(\xi_3)}{d\xi_3^2} + \left(k_0^2 \left(\varepsilon_{30} + \varepsilon_{3\Delta} \left(\frac{\xi_3 - \xi_{30}}{\xi_{30}} \right)^2 \right) - \frac{l(l+1)}{(a + \xi_3)^2} \right) \tilde{R}_{l_3}(\xi_3) = 0 \quad (111)$$

obtained after changing variables to the local coordinate ξ_3 . Using the approximation of Eq.(57) as well as the change of variables noted by Eq.(62), Eq.(111) becomes

$$\begin{aligned} \frac{d^2 \tilde{R}_{l_3}(x_3)}{dx_3^2} + \rho(l) \left[k_0^2 \varepsilon_{30} - \frac{l(l+1)}{a^2} \right] \tilde{R}_{l_3}(x_3) + \\ + \left[\rho(l) k_0^2 \varepsilon_{3\Delta} \left(\frac{x_3 - x_{30}}{x_{30}} \right)^2 + x_3 \right] \tilde{R}_{l_3}(x_3) = 0 \end{aligned} \quad (112)$$

where $\rho(l) \equiv (a^3 / (2l(l+1)))^{2/3}$. Defining

$$\left. \begin{aligned} k_{30}^2 &\equiv k_0^2 \varepsilon_{30}, & k_{3\Delta}^2 &\equiv k_0^2 \varepsilon_{3\Delta} \\ t_3(l) &\equiv -\rho(l) \left[k_{30}^2 - \frac{l(l+1)}{a^2} \right] \\ f_3(x_3, l) &\equiv \rho(l) k_{3\Delta}^2 \left(\frac{x_3 - x_{30}}{x_{30}} \right)^2 + x_3 \end{aligned} \right\} \quad (113)$$

Eq.(112) can be written as

$$\frac{d^2 \tilde{R}_l(x_3)}{dx_3^2} + (f_3(x_3, l) - t_3(l)) \tilde{R}_l(x_3) = 0 \quad (114)$$

Again, as was done in the procedure leading to Eq.(43), one needs to find the solution $l(l+1)$ to the equation

$$t_3(l) = \left(\frac{a^3}{2l(l+1)} \right)^{2/3} \left[\frac{l(l+1)}{a^2} - k_{30}^2 \right] \quad (115)$$

Hence, one has

$$l(l+1) \approx (k_{30}a)^2 \left[1 + \left(\frac{2}{k_{30}a} \right)^{2/3} t_3(l) \right], \quad t_3(l) \ll (k_{30}a)^{2/3} \quad (116)$$

Using the further approximation $l(l+1) \approx (k_{30}a)^2$, one can write

$$\rho(l) = \left(\frac{1}{k_{20}} \right)^2 \left(\frac{k_{30}a}{2} \right)^{2/3}, \quad x_3 = k_{30} \left(\frac{2}{k_{30}a} \right)^{1/3} \xi_3 \quad (117)$$

The function $f_3(x_3, l)$ now becomes

$$f_3(x_3, l) = f_3(x_3) = K \left(\frac{x_3 - x_{30}}{x_{30}} \right)^2 + x_3, \quad K \equiv \left(\frac{k_{30}a}{2} \right)^{2/3} \left(\frac{k_{3\Delta}}{k_{30}} \right)^2 \quad (118)$$

Equation (114) thus becomes

$$\frac{d^2 \tilde{R}_l(x_3)}{dx_3^2} + \left(K \left(\frac{x_3 - x_{30}}{x_{30}} \right)^2 + x_3 - t_3(l) \right) \tilde{R}_l(x_3) = 0 \quad (119)$$

Although Eq.(119) can be treated by ‘completing the square’ of the x_3 term, it proves to be more expeditious to perform a Taylor series expansion [25] about the minimum of $f_3(x_3)$. To this end, one has

$$f_3'(x_3) = \frac{2K}{x_{30}} \left(\frac{x_3 - x_{30}}{x_{30}} \right) + 1, \quad f_3''(x_3) = \frac{2K}{x_{30}^2} \quad (120)$$

The minimum x_{3m} of $f_3(x_3)$ occurs at $f_3'(x_{3m})=0$; hence, the first relation of Eq.(120) gives

$$x_{3m} = x_{30} \left(1 - \frac{x_{30}}{2K} \right) \quad (121)$$

Therefore,

$$f_3(x_{3m}) = x_{30} \left(1 - \frac{x_{30}}{4K} \right) \quad (122)$$

Thus, one has for the function $f_3(x_3)$

$$\begin{aligned} f_3(x_3) &= f_3(x_{3m}) + \frac{1}{2} f_3''(x_{3m})(x_3 - x_{3m})^2 \\ &= x_{30} \left(1 - \frac{x_{30}}{4K} \right) + \frac{1}{2} (x_3 - x_{3m})^2 f_3'' \end{aligned} \quad (123)$$

which gives, upon substitution into Eq.(114) and changing variables,

$$\frac{d^2 \tilde{R}_{l_3}(z_3)}{dz_3^2} + \left(\frac{1}{2} f_3'' z_3^2 - T_3(l) \right) \tilde{R}_{l_3}(z_3) = 0 \quad (124)$$

where $z_3 \equiv x_3 - x_{3m}$ and

$$T_3(l) \equiv t_3(l) - x_{30} \left(1 - \frac{x_{30}}{4K} \right) \quad (125)$$

Now, following Fock [25], consider the change of variables

$$\zeta = \left(2f_3'' \right)^{1/4} e^{-i\pi/4} z_3 \quad (126)$$

Equation (124) finally takes the form

$$\frac{d^2 \tilde{R}_{l_3}(\zeta)}{d\zeta^2} + \left(\nu + \frac{1}{2} - \left(\frac{1}{4} \right)^{\nu^2} \right) \tilde{R}_{l_3}(\zeta) = 0 \quad (127)$$

where

$$\nu + \frac{1}{2} \equiv -i \left(2f_3'' \right)^{1/2} T_3(l) \quad (128)$$

The solutions of the differential equation of Eq.(127) are parabolic cylinder functions D_ν of order ν [26, 27], viz.,

$$\tilde{R}_{l_3}(\zeta) = A_3 D_{-1-\nu}(i\zeta) + B_3 D_\nu(\zeta) \quad (129)$$

The behavior of this solution as $\zeta \rightarrow \infty$ renders the constant $A_3 = 0$. From Eqs.(126) and (120) and the definition of z_3 ,

$$\zeta = \alpha \left(\beta(r-a) - x_{3m} \right), \quad \alpha \equiv \left(\frac{4K}{x_{30}^2} \right)^{1/4} e^{-i\pi/4}, \quad \beta \equiv k_{30} \left(\frac{2}{k_{30}a} \right)^{1/3} \quad (130)$$

Thus, one has, from Eqs.(13) and (129), the scalar electric potential within the exosphere

$$U_{e_3}(r, \theta) = AB_3 \frac{D_\nu \left(\alpha \left(\beta(r-a) - x_{3m} \right) \right)}{r} P_l(-\cos\theta) \quad (131)$$

with ν given by the solution of Eq.(128). The associated electric and magnetic fields are given by, using Eqs.(10) and (11),

$$E_{\theta_3}(r, \theta) = AB_3 \left(\frac{1}{r} \right) \alpha \beta D'_\nu \left(\alpha \left(\beta(r-a) - x_{3m} \right) \right) \frac{\partial P_l(-\cos\theta)}{\partial \theta} \quad (132)$$

and

$$H_{\phi_3}(r, \theta) = ik_0 n_3^2 AB_3 \left(\frac{1}{r} \right) D_\nu \left(\alpha \left(\beta(r-a) - x_{3m} \right) \right) \frac{\partial P_l(-\cos\theta)}{\partial \theta} \quad (133)$$

Following the same process as before and equating these components at the boundary $r = a$ with those in region 2, using Eqs.(49) and (50), gives

$$AB_3 \alpha \beta D'_\nu(-\alpha x_{3m}) = ik_{l_2} A_2 \left[e^{ik_{l_2} \delta} - \frac{B_2}{A_2} e^{-ik_{l_2} \delta} \right] \quad (134)$$

and

$$An_3^2 B_3 D_\nu(-\alpha x_{3m}) = A_2 n_2^2 \left[e^{ik_{l_2} \delta} + \frac{B_2}{A_2} e^{-ik_{l_2} \delta} \right] \quad (135)$$

Here, remembering Eqs.(47), (55), and (116),

$$\kappa_{l_2} = (k_2^2 - k_{30}^2)^{1/2} \quad (136)$$

and

$$\frac{B_2}{A_2} = \frac{(k_2^2 - k_{30}^2)^{1/2} - k_2 \Delta_{12}}{(k_2^2 - k_{30}^2)^{1/2} + k_2 \Delta_{12}} \quad (137)$$

with Δ_{12} given by Eq.(54). Taking the ratio of Eqs.(134) and (135) gives the modal equation

$$D'_\nu(-\alpha x_{3m}) - q D_\nu(-\alpha x_{3m}) = 0 \quad (138)$$

where

$$q \equiv i \left(\frac{\varepsilon_3}{\varepsilon_2} \right) (k_2^2 - k_{30}^2)^{1/2} \left(\frac{x_{30}^2}{4K} \right)^{1/4} \left(\frac{1}{k_{30}} \right) \left(\frac{k_{30} a}{2} \right)^{1/3} e^{i\pi/4} \frac{\left[e^{i\kappa_{l_2} \delta} - \frac{B_2}{A_2} e^{-i\kappa_{l_2} \delta} \right]}{\left[e^{i\kappa_{l_2} \delta} + \frac{B_2}{A_2} e^{-i\kappa_{l_2} \delta} \right]} \quad (139)$$

The solution of Eq.(138) for the propagation modes within the exosphere is not with respect to the arguments $-\alpha x_{3m}$ for they are specified by the problem; the solution is with respect to the order ν . These spectra of values ν_j are then used in Eqs.(128) and (125) to determine the corresponding values of t_{3j} for use with Eq.(116).

Normalizing the radial solution given by Eq.(129) (with $A_3 = 0$) at the boundary $r = a$ yields

$$\tilde{R}_{l_3}(a) = B_3 D_\nu(-\alpha x_{3m}) = 1 \quad (140)$$

Hence, the full solution for the electric scalar potential is, using Eq.(131), and noting that one is dealing with an array of modal values ν_j

$$U_{e_3}(r, \theta) = \sum_{j=1}^{\infty} A_j \frac{D_{\nu_j}(\alpha(\beta(r-a) - x_{3m}))}{D_{\nu_j}(-\alpha x_{3m})} \left(\frac{1}{r} \right) P_l(-\cos \theta) \quad (141)$$

As before, the values of the amplitudes A_j of the modes supported along the lunar surface will be determined by the boundary value problem defined by the source of the electromagnetic radiation within the exosphere.

i. Derivation of the Equation for the Modal Amplitudes Within the Exosphere

The procedure to obtain the values of the modal amplitudes will follow along the same lines as established in Section III.d.i above. Thus, one attempts to decouple the amplitudes A_j from the sum of Eq.(141) by forming the integral

$$\begin{aligned} \int_0^{\infty} r U_{e_3}(r, \theta) \frac{D_{\nu_{j'}}(\alpha(\beta \xi_3 - x_{3m}))}{D_{\nu_{j'}}(-\alpha x_{3m})} d\xi_3 \frac{1}{P_l(-\cos \theta)} = \\ = \sum_{j=1}^{\infty} A_j \int_0^{\infty} \frac{D_{\nu_{j'}}(\alpha(\beta \xi_3 - x_{3m}))}{D_{\nu_{j'}}(-\alpha x_{3m})} \frac{D_{\nu_j}(\alpha(\beta \xi_3 - x_{3m}))}{D_{\nu_j}(-\alpha x_{3m})} d\xi_3 \end{aligned} \quad (142)$$

and attempt to ascertain the orthogonality of the parabolic cylinder functions appearing on the right side using the established properties of these functions dictated by the problem at hand; that is, the defining equation of Eq.(127),

$$\frac{d^2 D_{\nu_j}(\zeta)}{d\zeta^2} + \left(\nu_j + \frac{1}{2} - \left(\frac{1}{4}\right)\zeta^2 \right) D_{\nu_j}(\zeta) = 0 \quad (143)$$

and the condition of Eq.(138)

$$\left. \frac{dD_{\nu_j}(\zeta)}{d\zeta} - q D_{\nu_j}(\zeta) \right|_{\zeta = -\alpha x_{3m}} = 0 \quad (144)$$

Thus, the procedure established in III.d.i will be followed; multiplying Eq.(143) by $D_{\nu_{j'}}(\zeta)$ and subtracting from this result Eq.(143) for $\nu_{j'}$ multiplied by $D_{\nu_j}(\zeta)$, changing variables using $\zeta = \alpha\beta z_3 - \alpha x_{3m}$, integrating with respect to z_3 , and performing an integration by parts on the portion with the derivatives yields

$$\frac{1}{\alpha\beta} \left(D_{\nu_{j'}}(\zeta) \frac{dD_{\nu_j}(\zeta)}{d\zeta} - D_{\nu_j}(\zeta) \frac{dD_{\nu_{j'}}(\zeta)}{d\zeta} \right) \Bigg|_{z_3=0}^{\infty} = (\nu_{j'} - \nu_j) \int_0^{\infty} D_{\nu_{j'}}(\zeta) D_{\nu_j}(\zeta) dz_3 \quad (145)$$

Using Eq.(144), this gives

$$\int_0^{\infty} D_{\nu_{j'}}(\zeta) D_{\nu_j}(\zeta) dz_3 = 0, \quad \nu_j \neq \nu_{j'} \quad (146)$$

In the event that $\nu_j = \nu_{j'}$, one has from Eq.(145) upon applying L'Hospital's rule

$$\lim_{\nu_{j'} \rightarrow \nu_j} \int_0^{\infty} D_{\nu_{j'}}(\zeta) D_{\nu_j}(\zeta) dz_3 = \frac{1}{\alpha\beta} \lim_{\nu_{j'} \rightarrow \nu_j} \left(\frac{dD_{\nu_{j'}}(\zeta)}{d\nu_{j'}} \frac{dD_{\nu_j}(\zeta)}{d\zeta} - D_{\nu_j}(\zeta) \frac{d^2 D_{\nu_{j'}}(\zeta)}{d\nu_{j'} d\zeta} \right) \Bigg|_{z_3=0}^{\infty} \quad (147)$$

The connection between ζ and $\nu_{j'}$ is given through $y \equiv \nu_{j'} + 1/2 - (1/4)\zeta^2$; hence, $d/d\zeta = -\left(\frac{1}{2}\zeta\right)^{-1} d/d\nu_{j'}$. Using this in Eq.(147) and employing Eqs.(143) and (144) finally gives

$$\begin{aligned} \int_0^{\infty} D_{\nu_j}^2(\zeta) dz_3 &= -\frac{1}{\alpha\beta} \left(\frac{2}{\zeta} \right) \left(q^2 D_{\nu_j}^2(\zeta) + D_{\nu_j}(\zeta) \left\{ \nu_j + \frac{1}{2} - \left(\frac{1}{4}\zeta^2\right) \right\} D_{\nu_j}(\zeta) \right) \Bigg|_{z_3=0}^{\infty} \\ &= \left(\frac{1}{\alpha\beta} \right) \left(\frac{2}{\alpha x_{3m}} \right) \left(\left(\frac{1}{4}\right) (\alpha x_{3m})^2 - \left(\nu_j + \frac{1}{2}\right) - q^2 \right) P_{\nu_j}^2(-\alpha x_{3m}) \end{aligned} \quad (148)$$

Hence, using the results of Eqs.(146) and (148) in Eq.(142) gives for the modal amplitudes

$$\begin{aligned} A_j &= \alpha\beta \left(\frac{\alpha x_{3m}}{2} \right) \left(\frac{1}{\left(\frac{1}{4}\right) (\alpha x_{3m})^2 - \left(\nu_j + \frac{1}{2}\right) - q^2} \right) \frac{1}{P_l(-\cos\theta)} \cdot \\ &\quad \cdot \int_0^{\infty} r U_{e_3}(r, \theta) \frac{D_{\nu_j}(\alpha(\beta \xi_3^2 - x_{3m}))}{D_{\nu_j}(-\alpha x_{3m})} d\xi_3 \end{aligned} \quad (149)$$

ii. Evaluation of the Modal Amplitudes for a Given Source Distribution

The source of the electromagnetic radiation in the lunar exosphere is again taken to be a vertical electric dipole, the electric scalar potential of which is given by Eq.(88). Applying this relation to that of Eq.(149) and following the procedure given in Section III.d.ii, one has for $\theta \rightarrow 0$,

$$\int_0^{\infty} r U_{e_3}(r, \theta) \frac{D_{\nu_j}(\alpha(\beta \xi_3^2 - x_{3m}))}{D_{\nu_j}(-\alpha x_{3m})} d\xi_3 \approx i \left(\frac{JL}{\omega} \right) \frac{D_{\nu_j}(\alpha(\beta(r_s - a) - x_{3m}))}{D_{\nu_j}(-\alpha x_{3m})} (-\ln\theta^2) \quad (150)$$

Substituting Eq.(150) into Eq.(149) and using Eq.(94) gives for the modal amplitudes

$$A_j = -\frac{i}{2} \left(\frac{\pi \alpha^2 \beta x_{3m}}{\sin \pi l} \right) \left(\frac{JL}{\omega} \right) \left(\frac{1}{\left(\frac{1}{4} \right) (\alpha x_{3m})^2 - \left(\nu_j + \frac{1}{2} \right) - q^2} \right) \frac{D_{\nu_j} \left(\alpha \left(\beta (r_s - a) - x_{3m} \right) \right)}{D_{\nu_j} \left(-\alpha x_{3m} \right)} \quad (151)$$

iii. The Electric Scalar Potential and Associated Radial Electric Field

Substituting Eq.(151) into Eq.(141) gives for the scalar electric potential in the lunar exosphere

$$U_{e_3}(r, \theta) = -\frac{i}{2} \left(\frac{\pi \alpha^2 \beta x_{3m}}{\sin \pi l} \right) \left(\frac{JL}{\omega} \right) \sum_{j=1}^{\infty} \left(\frac{1}{\left(\frac{1}{4} \right) (\alpha x_{3m})^2 - \left(\nu_j + \frac{1}{2} \right) - q^2} \right) \cdot \frac{D_{\nu_j} \left(\alpha \left(\beta (r_s - a) - x_{3m} \right) \right) D_{\nu_j} \left(\alpha \left(\beta (r - a) - x_{3m} \right) \right)}{D_{\nu_j} \left(-\alpha x_{3m} \right) D_{\nu_j} \left(-\alpha x_{3m} \right)} \left(\frac{1}{r} \right) P_l(-\cos \theta) \quad (152)$$

Using Eqs.(97), (99), and (100) in Eq.(152), and employing the definitions for α and β yields

$$U_{e_3}(r, \theta) = (2\pi)^{1/2} e^{i\pi/4} k_{30} \left(\frac{2}{k_{30}a} \right)^{1/3} K^{1/2} \left(\frac{x_{3m}}{x_{30}} \right) \left(\frac{JL}{\omega} \right) \left(\frac{1}{k_{30}a \sin \theta} \right)^{1/2} e^{ik_{30}a\theta} \left(\frac{1}{r} \right) \cdot \sum_{j=1}^{\infty} \left(\frac{1}{\left(\frac{1}{4} \right) (\alpha x_{3m})^2 - \left(\nu_j + \frac{1}{2} \right) - q^2} \right) \frac{D_{\nu_j} \left(\alpha \left(\beta (r_s - a) - x_{3m} \right) \right) D_{\nu_j} \left(\alpha \left(\beta (r - a) - x_{3m} \right) \right)}{D_{\nu_j} \left(-\alpha x_{3m} \right) D_{\nu_j} \left(-\alpha x_{3m} \right)} e^{ix(\theta)t_{3j}} \quad (153)$$

where, from Eqs.(125) and (128),

$$t_{3j} = i \frac{(4K)^{1/2}}{x_{30}} \left(\nu_j + \frac{1}{2} \right) + x_{30} \quad (154)$$

The associated electric field for this scalar potential is given by Eq.(104); substituting Eq.(153) into Eq.(104) yields for the radial electric field within the exosphere

$$E_{r_3}(r, \theta) = (2\pi)^{1/2} e^{i\pi/4} k_{30} (k_{30}a)^2 \left(\frac{2}{k_{30}a} \right)^{1/3} K^{1/2} \left(\frac{x_{3m}}{x_{30}} \right) \left(\frac{JL}{\omega} \right) \left(\frac{1}{k_{30}a \sin \theta} \right)^{1/2} e^{ik_{30}a\theta} \left(\frac{1}{r} \right)^2 \cdot \sum_{j=1}^{\infty} \left(\frac{1}{\left(\frac{1}{4} \right) (\alpha x_{3m})^2 - \left(\nu_j + \frac{1}{2} \right) - q^2} \right) \frac{D_{\nu_j} \left(\alpha \left(\beta (r_s - a) - x_{3m} \right) \right) D_{\nu_j} \left(\alpha \left(\beta (r - a) - x_{3m} \right) \right)}{D_{\nu_j} \left(-\alpha x_{3m} \right) D_{\nu_j} \left(-\alpha x_{3m} \right)} e^{ix(\theta)t_{3j}} \quad (155)$$

Finally, letting ξ_{3_r} be the distance from the lunar surface to the point of reception, i.e., $\xi_{3_r} = r - a$, and $r^{-2} = (\xi_{3_r} + a)^{-2} \approx a^{-2}$ with $\xi_{3_s} = r_s - a$, Eq. (155) gives, after rearrangement of factors and simplification

$$E_{r_3}(\xi_{3_r}, \theta) = E_0(\theta) V(x(\theta), \xi_{3_s}, \xi_{3_r}, q) \quad (156)$$

where the attenuation factor is

$$V(x(\theta), \xi_{3_s}, \xi_{3_r}, q) \equiv -2ie^{i\pi/4} K^{1/2} (\pi x(\theta))^{1/2} \left(\frac{x_{3m}}{x_{30}} \right) \cdot \sum_{j=1}^{\infty} \left(\frac{1}{\left(\frac{1}{4}\right)(\alpha x_{3m})^2 - (\nu_j + 1/2) - q^2} \right) \frac{D_{\nu_j}(\alpha(\beta \xi_{3_s} - x_{3m})) D_{\nu_j}(\alpha(\beta \xi_{3_r} - x_{3m}))}{D_{\nu_j}(-\alpha x_{3m}) D_{\nu_j}(-\alpha x_{3m})} e^{ix(\theta)t_{3_j}} \quad (157)$$

and the non-diffractive field strength is

$$E_0(\theta) \equiv ik_{30}^2 \left(\frac{JL}{\omega} \right) \frac{e^{ik_{30}a\theta}}{a(\theta \sin \theta)^{1/2}} \quad (158)$$

Equations (156)–(158) describe radio wave propagation within the lunar exosphere and takes into account diffraction around the surface of the moon as well as the effect of the regolith.

iv. Numerical Evaluation of the Modal Equation and of the Electric Field

At the outset, one must evaluate the spectrum of roots ν_j that satisfy Eq.(138). To this end, it is required to provide a method for the evaluation of the derivative $D'_\nu(\dots)$ since *Mathematica* does not supply a routine as it does for the derivative of the Airy functions. To circumvent this, one can use recursion relationships that prevail for the parabolic cylinder functions [28], viz.,

$$D'_\nu(x) + \left(\frac{1}{2}\right)x D_\nu(x) - \nu D_{\nu-1}(x) = 0, \quad D'_\nu(x) - \left(\frac{1}{2}\right)x D_\nu(x) + D_{\nu+1}(x) = 0 \quad (159)$$

Adding these two relationships, solving for $D'_\nu(x)$ and using this result in Eq.(138) gives for the modal equation,

$$\nu D_{\nu-1}(-\alpha x_{3m}) - D_{\nu+1}(-\alpha x_{3m}) - 2q D_\nu(-\alpha x_{3m}) = 0 \quad (160)$$

which must be solved for ν . As done before, the contours of the real and imaginary parts of this equation will be plotted with respect to the parameters σ and τ where

$$\nu_j = \sigma_j + i\tau_j \quad (161)$$

are the roots of Eq.(160) where the two contours intersect.

As an example, consider an operating frequency of 500 KHz (sufficiently above the 220 KHz cutoff frequency as shown in Fig. 3.). Taking a the regolith thickness of $\delta = 50$ m, and using the parameters discussed in Section II.b, one finds, upon implementing Eqs.(8), (54), (137) & (139)

$$q = -3.289 - 0.210i \quad (162)$$

Using this and the corresponding values of α and x_{3m} in Eq.(160) yields the following contour plot for the roots ν_j of the equation as shown in Fig. 11. The first root is noted to occur at $\nu_1 = -0.637 - 0.658i$. Here, one must be careful that the roots ν_j chosen are such that, using Eq.(154), $\text{Im} \{t_{3j}\} > 0$ so as to have a solution that decays with $e^{ix(\theta)t_{3j}}$. In this case, ν_1 is such that $\text{Im} \{t_{31}\} < 0$. Hence, this root is an extraneous one and must be neglected. The second root $\nu_2 = -0.357 + 0.378i$ satisfies the corresponding $\text{Im} \{t_{32}\} > 0$ and thus becomes the first root of the mode spectrum ν_j and is the dominant mode.

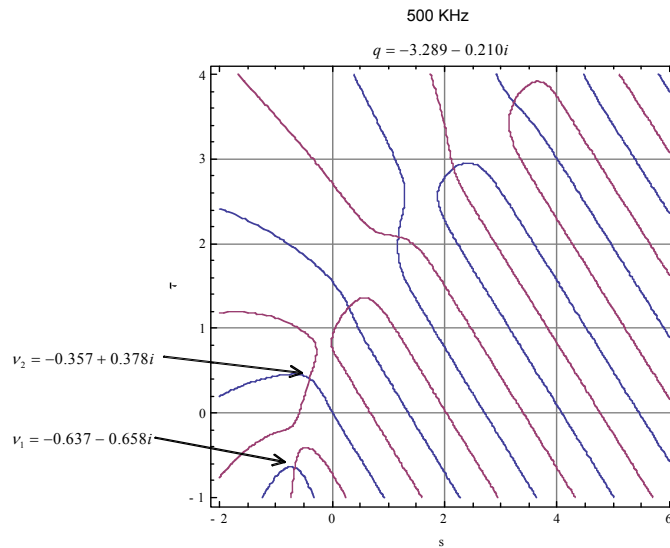


Figure 11. Real (σ) and Imaginary (τ) Parts of the Orders ν of Eq.(138).

As before, assume a transmitter height above the lunar surface to be 20 m and that of the receiver to be 2 m; the transmitter output power into the 10 m length dipole is 1 W. Taking the three regolith thicknesses of $\delta = 0$ m, $\delta = 50$ m, and $\delta = 100$ m, and using

Eqs.(139), (160), (154), and (156) yields the results shown in Fig. 12. Here again, the electric field strength in volts/meter is plotted versus propagation distance in kilometers along the lunar surface. The deleterious effect of the regolith, similar to the case of Fig. 9, is seen.

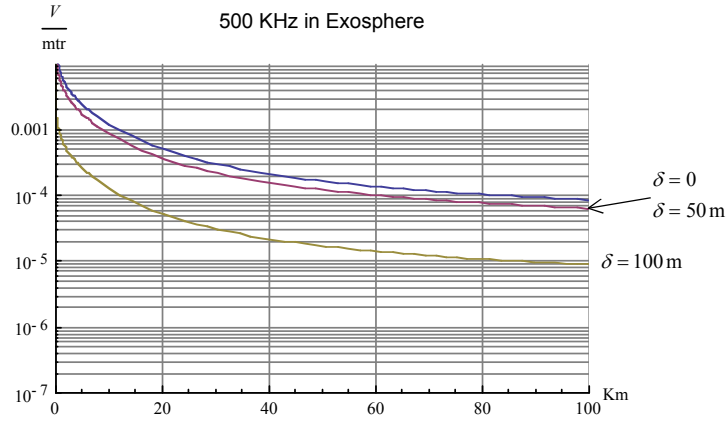


Figure 12. Electric Field Strength vs. Distance Along Lunar Surface at 500 KHz

The behavior of the effect of the regolith is the same as it is for the case of no exospheric plasma save for the fact that the field strengths are more than an order of magnitude greater for the exospheric case. The 1 MHz example shown in Fig 13 again follows that of Fig. 10 for the case of no exospheric plasma. Thus, the existence of the regolith is deleterious to radio wave propagation along the lunar surface in the presence of an exosphere.

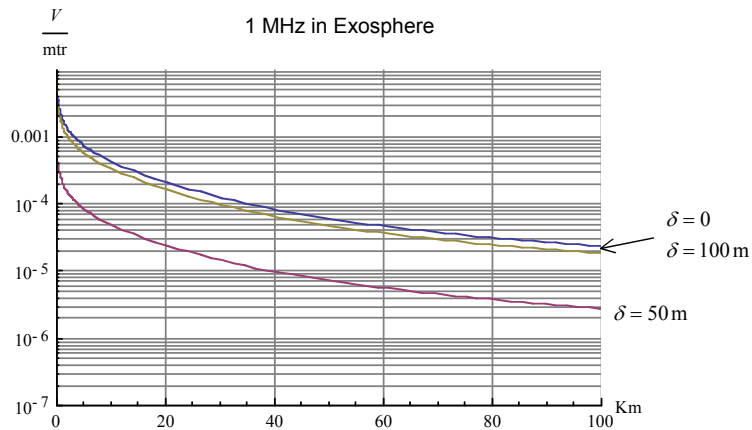


Figure 13. Electric Field Strength vs. Distance Along Lunar Surface at 1 MHz

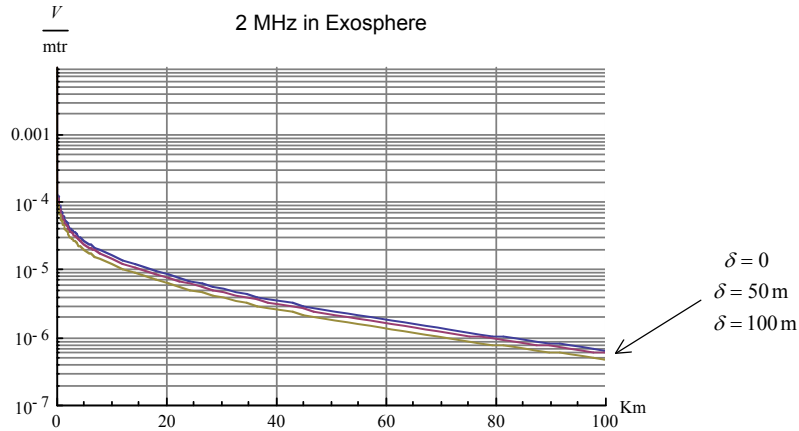


Figure 14. Electric Field Strength vs. Distance Along Lunar Surface at 2 MHz

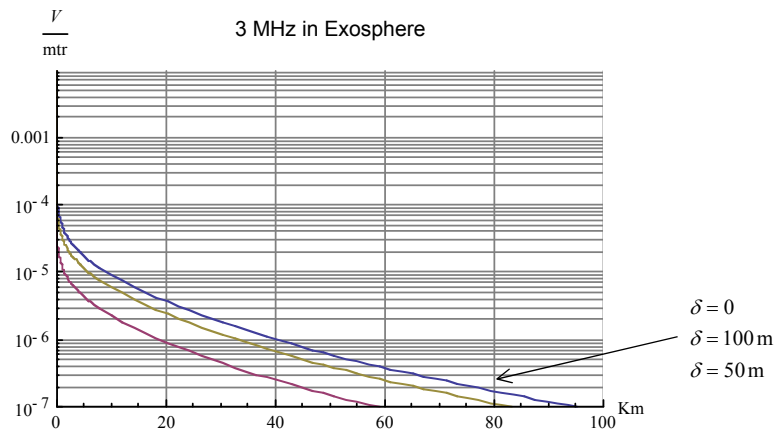


Figure 15. Electric Field Strength vs. Distance Along Lunar Surface at 3 MHz

For 2 MHz shown in Fig. 14, all regolith examples perform about the same whereas for 3 MHz shown in Fig. 15, the cases again separate in which the regolith attenuates the wave as compared to the case of $\delta = 0$.

IV. Conclusions and Discussion

It has been shown in the examples considered in this study that the presence of a lunar regolith is deleterious to transhorizon radio wave propagation above frequencies of 100 KHz. However, when an exospheric plasma is present, the cutoff frequency for communications is ~ 200 KHz, below which electromagnetic waves do not propagate through the plasma. Thus, unless the exospheric plasma is nonexistent, the lunar regolith provides no advantages for surface wave propagation. However, the exospheric plasma

as assumed here does actively support long-range transhorizon communications for frequencies from 500 KHz to 2 MHz, the lower frequencies being favored over the larger ones. Given the fact that the 500 KHz frequency is close to that of the exospheric plasma frequency, and allowing for variations of the plasma properties as assumed in Section II.d, it would be a reliable choice to employ communications frequencies ~ 1 MHz for lunar transhorizon communications.

These conclusions, however, are based on an exosphere model composed essentially of one data point, i.e., the data of Fig. 2. It is clear that much more information of the exosphere is needed before reliable communications system predictions can be made. For example, the variation of electron concentration with respect to height linked to the spatial variation across the dayside surface of the moon is required. Some very early considerations of these points can be found in the literature [29]. The exosphere model of Section II.b and the propagation model of Section III.e are general enough to accommodate a wide range of exosphere scenarios. Additionally, information of the lunar regolith in terms of its spatial variation with respect to displacements along the lunar surface as well as its electrical properties and that of the core material is needed to assess the impact on surface wave propagation. Finally, it must be remembered that the examples given here are for the worst case of an electrically small vertical electric dipole operating at 1 W. The use of a directional transmitting antenna and larger power will, of course, substantially improve performance.

Although there is much data to be obtained, this study demonstrates the potential for low frequency, long-range transhorizon communication along the lunar surface and provides an analysis procedure for its assessment. It hopefully will provide impetus for further investigation and consideration for low data rate communications for contingency purposes during lunar exploration activities.

References

1. D. S. McKay, "Evolution of the Lunar Regolith", in *The Lunar Regolith Simulant Materials Workshop*, Marshall Institute, January 24-26, 2005, L. Sibille and P. Carpenter, eds., pp. 5-7.
2. D. L. Reasoner, and W. J. Burke, "Direct Observations of the Lunar Photoelectron Layer", *Geochim. Cosmochim. Acta Suppl.* **3**, pp. 2639-2654 (1972).
3. A. S. Vyshlov, "Preliminary Results of Circum-Lunar Plasma Research by the Luna 22 Spacecraft", *Space Research* **16**, pp. 945-949 (1974).
4. S. J. Bauer, "Limits to a Lunar Ionosphere", *Anzeiger Abt. II* **133**, pp. 17-21 (1996).
5. T. Hagfors, "Remote Probing of the Moon by Infrared and Microwave Emissions and by Radar", *Radio Sci.* **5** (2), pp. 189-227 (1970).
6. N. F. Ness, K. W. Behannon, C. S. Scarce, and S. C. Cantarano, "Early Results from the Magnetic Field Experiment on Lunar Explorer 35", *J. Geophys. Res.* **72**, pp. 5769-5778 (1967).

7. V. A. Bader, O. I. Yakovlev, and P. Novichikhin, "The Propagation of Radio Waves Along the Lunar Surface", *Radio Eng. Electron Phys.* **22** (10), pp. 63-67 (1977).
8. See, for example, V. L. Ginzburg, *Propagation of Electromagnetic Waves in Plasma* (Gordon & Breach, New York, 1961), p. 26.
9. G. Arfkin, *Mathematical Methods for Physicists*, 3rd ed. (Academic Press, New York, 1985), p. 623.
10. J. Galjes, *Terrestrial Propagation of Long Electromagnetic Waves* (Pergamon Press, New York, 1972), pp. 88.
11. M. Abramowitz and I. A. Stegun, eds., *Handbook of Mathematical Functions* (Dover, New York, 1972), p. 446.
12. V. A. Fock, *Electromagnetic Diffraction and Propagation Problems* (New York, Pergamon Press, 1965). Appendix.
13. L. W. Pearson, "A Scheme for Automatic Computation of Fock-Type Integrals", *IEEE Trans. Antennas, Propagat.* **35** (10), pp. 1111-1118 (1987). Appendix.
14. J. C. P. Miller, "The Airy Integral", in *British Assoc. for the Advancement of Science, Mathematical Tables (Part-Vol B.)* (Cambridge University Press, 1946).
15. A. N. Sommerfeld, "Über die Ausbreitung der Wellen in der Drachtlosen Telegraphie" (English Trans: "Propagation of Waves in Wireless Telegraphy"), *Ann. Physik* **81**, pp. 1135-1153 (1926).
16. J. R. Wait, *Electromagnetic Waves in Stratified Media* (Pergamon Press, New York, 1962). P.160.
17. Ref. 16, p. 175.
18. N. N. Lebedev, *Special Functions and Their Applications*, (Dover, New York, 1972), p.201.
19. Ref 18, p. 53.
20. Ref. 10, p. 83.
21. Ref. 12, p. 206.
22. Ref. 12, p. 207 & 239.
23. Ref. 12, p. 240.
24. P. V. Bliokh, A. P. Nicholaenko, and Yu. F. Fillippov, *Schumann Resonances in the Earth-Ionosphere Cavity*, (IEE, London, 1980). Chap.2.
25. Ref. 12, pp. 315-320.
26. A. Erde'lyi, *Higher Transcendental functions* (McGraw-Hill, New York, 1953). Vol. 2, Chap. 8.
27. Ref. 11, Chap. 19.
28. Ref. 27, p. 688, Eqs.(19.6.1) & (19.6.2).
29. H. Weil and M. L. Barasch, "A Theoretical Lunar Ionosphere", *Icarus* **1**, pp. 346-356 (1963).

Appendix A

Derivation of the Electromagnetic Field Components in Terms of A Scalar Potential for TM (Electric) Waves

By way of a brief review, the components of the electric and magnetic field vectors of a propagating wave field along a spherical planet or moon will each be related to a single scalar potential. The particular case for transverse-magnetic (TM) waves, or electric waves, will be considered. The equations derived in this Appendix will form the basis of analysis of electromagnetic wave propagation in a spherically layered environment.

The Maxwell Equations in traditional cgs units are given by

$$\bar{\nabla} \times \bar{H} - \frac{1}{c} \frac{\partial \bar{D}}{\partial t} = \frac{4\pi}{c} \bar{j} \quad (\text{A1})$$

$$\bar{\nabla} \times \bar{E} + \frac{1}{c} \frac{\partial \bar{B}}{\partial t} = 0 \quad (\text{A2})$$

$$\bar{\nabla} \cdot \bar{D} = 4\pi\rho \quad (\text{A3})$$

$$\bar{\nabla} \cdot \bar{B} = 0 \quad (\text{A4})$$

which relate the electric and magnetic field intensities, \bar{E} and \bar{B} , to the electric and magnetic inductions, \bar{D} and \bar{B} , in the presence of an external current \bar{j} and charge density ρ . Associated with these are the constitutive relationships involving the prevailing electric permittivity ε , the magnetic permeability μ , and the conductivity σ , viz,

$$\bar{D} = \varepsilon\bar{E}, \quad \bar{B} = \mu\bar{H}, \quad \bar{j} = \sigma\bar{E} \quad (\text{A5})$$

In the propagation situations considered here, one has $\rho=0$ and $\mu=1$. Using Eqs.(A5) in Eqs.(A1)-(A4) with these values gives

$$\bar{\nabla} \times \bar{H} - \frac{\varepsilon}{c} \frac{\partial \bar{E}}{\partial t} = \frac{4\pi}{c} \sigma\bar{E} \quad (\text{A6})$$

$$\bar{\nabla} \times \bar{E} + \frac{1}{c} \frac{\partial \bar{H}}{\partial t} = 0 \quad (\text{A7})$$

$$\bar{\nabla} \cdot \bar{E} = 0 \quad (\text{A8})$$

$$\bar{\nabla} \cdot \bar{H} = 0 \quad (\text{A9})$$

Furthermore, the field components $\vec{E}(\vec{r}, t)$ and $\vec{H}(\vec{r}, t)$ are taken to be time harmonic,

$$\vec{E}(\vec{r}, t) = \vec{E}'(\vec{r}) \exp(-i\omega t) \quad (\text{A10})$$

$$\vec{B}(\vec{r}, t) = \vec{B}'(\vec{r}) \exp(-i\omega t) \quad (\text{A11})$$

Substituting Eqs.(A10) and (A11) in Eqs.(A6)-(A9) yields

$$\vec{\nabla} \times \vec{H}' + i \frac{\omega}{c} \varepsilon \vec{E}' = \frac{4\pi}{c} \sigma \vec{E}' \quad (\text{A12})$$

$$\vec{\nabla} \times \vec{E}' - i \frac{\omega}{c} \vec{H}' = 0 \quad (\text{A13})$$

$$\vec{\nabla} \cdot \vec{E}' = 0 \quad (\text{A14})$$

$$\vec{\nabla} \cdot \vec{H}' = 0 \quad (\text{A15})$$

In this case, Eqs.(A14) and (A15) are essentially the result from Eqs.(A12) and (A13); hence, the former will be omitted from further treatment. Thus, the working relationships for the electric and magnetic fields are

$$\vec{\nabla} \times \vec{H}' = \left(\frac{4\pi}{c} \sigma - i \frac{\omega}{c} \varepsilon \right) \vec{E}' \quad (\text{A16})$$

$$\vec{\nabla} \times \vec{E}' = +i \frac{\omega}{c} \vec{H}' \quad (\text{A17})$$

In order to capture the essence of the parameters in these equations and their impact on wave propagation, it is beneficial to obtain the wave equation from Eqs.(A16) and (A17); in the usual way, one obtains from Eq.(A17)

$$\vec{\nabla} \times \vec{\nabla} \times \vec{E}' = \vec{\nabla} (\vec{\nabla} \cdot \vec{E}') - \nabla^2 \vec{E}' = +i \frac{\omega}{c} \vec{\nabla} \times \vec{H}' \quad (\text{A18})$$

Using Eqs.(A14) and (A16) and rearranging terms results in

$$\nabla^2 \vec{E}' + k^2 \vec{E}' = 0 \quad (\text{A19})$$

where

$$k = k_0 \left(\varepsilon + i \frac{4\pi\sigma}{\omega} \right)^{1/2} \equiv k_0 n \quad (\text{A20})$$

Here, $k_0 \equiv \omega/c$ is the free-space wave number and n is the refractive index of the propagation medium.

Given these considerations, Eqs.(A16) and (A17) can be written

$$\bar{\nabla} \times \bar{H}' = -ik_0 n^2 \bar{E}' \quad (\text{A21})$$

$$\bar{\nabla} \times \bar{E}' = +ik_0 \bar{H}' \quad (\text{A22})$$

It is from these two relations that one can obtain individual expressions for each of the six components comprising the electric and magnetic field vector components solely in terms of two scalar functions, the electric and magnetic potentials. To this end, the solution in terms of the electric potential for a problem in spherical coordinates will be found. In spherical coordinates,

$$\begin{aligned} \bar{\nabla} \times \bar{H}' = & \left(\frac{1}{r^2 \sin \theta} \right) \left\{ \frac{\partial}{\partial \theta} (r \sin \theta H_\phi) - \frac{\partial}{\partial \phi} (r H_\theta) \right\} \hat{r} - \\ & -r \left\{ \frac{\partial}{\partial r} (r \sin \theta H_\phi) - \frac{\partial}{\partial \phi} H_r \right\} \hat{\theta} + r \sin \theta \left\{ \frac{\partial}{\partial r} (r H_\theta) - \frac{\partial}{\partial \theta} H_r \right\} \hat{\phi} \end{aligned} \quad (\text{A23})$$

where \hat{r} , $\hat{\theta}$, and $\hat{\phi}$ are the unit vectors in the radial, colatitude, and azimuthal directions, respectively, and H_r , H_θ , and H_ϕ are the associated magnetic field components. Hence, the components of Eq.(A21) are

$$-ik_0 n^2 E_r = \left(\frac{1}{r \sin \theta} \right) \left[\frac{\partial}{\partial \theta} (\sin \theta H_\phi) - \frac{\partial}{\partial \phi} H_\theta \right] \quad (\text{A24})$$

$$-ik_0 n^2 E_\theta = \left(\frac{1}{r \sin \theta} \right) \left[\frac{\partial H_r}{\partial \phi} - \frac{\partial}{\partial r} (r \sin \theta H_\phi) \right] \quad (\text{A25})$$

$$-ik_0 n^2 E_\phi = \left(\frac{1}{r} \right) \left[\frac{\partial}{\partial r} (r H_\theta) - \frac{\partial H_r}{\partial \theta} \right] \quad (\text{A26})$$

Similarly, for Eq.(A22), one obtains

$$-ik_0 H_r = \left(\frac{1}{r \sin \theta} \right) \left[\frac{\partial E_\theta}{\partial \phi} - \frac{\partial}{\partial \theta} (\sin \theta E_\phi) \right] \quad (\text{A27})$$

$$-ik_0 H_\theta = \left(\frac{1}{r \sin \theta} \right) \left[\frac{\partial}{\partial r} (r \sin \theta E_\phi) - \frac{\partial E_r}{\partial \phi} \right] \quad (\text{A28})$$

$$-ik_0 H_\phi = \left(\frac{1}{r}\right) \left[\frac{\partial E_r}{\partial \theta} - \frac{\partial}{\partial r} (rE_\theta) \right] \quad (\text{A29})$$

The object now is to essentially decouple these relations to obtain explicit equations for each of the separate field components. The process commences with limiting the analysis to fields of transverse magnetic type (i.e., electric waves) in which $H_r = 0$ and $E_r \neq 0$. (A similar procedure can be done for the transverse electric case in which $E_r = 0$ and $H_r \neq 0$ but this is not of interest in this work.)

With $H_r = 0$, Eqs.(A25)-(A27) simplify to

$$-ik_0 n^2 E_\theta = -\left(\frac{1}{r}\right) \frac{\partial}{\partial r} (rH_\phi) \quad (\text{A30})$$

$$-ik_0 n^2 E_\phi = \left(\frac{1}{r}\right) \frac{\partial}{\partial r} (rH_\theta) \quad (\text{A31})$$

$$\frac{\partial E_\theta}{\partial \phi} = \frac{\partial}{\partial \theta} (\sin \theta E_\phi) \quad (\text{A32})$$

The only way Eq.(A32) is satisfied is if there exists a scalar function Φ such that

$$\sin \theta E_\phi = \frac{\partial \Phi}{\partial \phi}, \quad E_\theta = \frac{\partial \Phi}{\partial \theta} \quad (\text{A33})$$

Using the second relation of Eq.(33) in Eq.(30) yields

$$-ik_0 n^2 \frac{\partial \Phi}{\partial \theta} = -\left(\frac{1}{r}\right) \frac{\partial}{\partial r} (rH_\phi) \quad (\text{A34})$$

Multiplying Eq.(30) by $\sin \theta$ and using the first relation of Eq.(33) gives

$$-ik_0 n^2 \frac{\partial \Phi}{\partial \phi} = \frac{\sin \theta}{r} \frac{\partial}{\partial r} (rH_\theta) \quad (\text{A35})$$

Now assume there exists another scalar function ψ such that $\Phi = \frac{1}{r} \frac{\partial \psi}{\partial r}$. This allows Eqs.(A34) and (A35) to become

$$H_\phi = + \frac{ik_0 n^2}{r} \frac{\partial \psi}{\partial \theta} \quad (\text{A36})$$

and

$$H_\theta = -\frac{ik_0 n^2}{r \sin \theta} \frac{\partial \psi}{\partial \phi} \quad (\text{A37})$$

Finally, it is convenient to rescale the function ψ by $1/r$, i.e., consider the scalar $U_e = \frac{\psi}{r}$. Equations (A36) and (A37) then simplify to

$$H_\phi = +ik_0 n^2 \frac{\partial U_e}{\partial \theta} \quad (\text{A38})$$

and

$$H_\theta = -\frac{ik_0 n^2}{\sin \theta} \frac{\partial U_e}{\partial \phi} \quad (\text{A39})$$

These two magnetic field components are now given in terms of the electric potential, U_e . Given these, they can now be used in Eqs.(A24), (A30), and (A31) to obtain similar expressions for E_r , E_θ , and E_ϕ :

$$E_r = -\frac{1}{r \sin \theta} \left[\frac{\partial}{\partial \theta} \left(\sin \theta \frac{\partial U_e}{\partial \theta} \right) + \frac{\partial}{\partial \phi} \left(\frac{1}{\sin \theta} \frac{\partial U_e}{\partial \phi} \right) \right] \quad (\text{A40})$$

$$E_\theta = \frac{1}{r} \frac{\partial}{\partial r} \left(r \frac{\partial U_e}{\partial \theta} \right) \quad (\text{A41})$$

$$E_\phi = \left(\frac{1}{r \sin \theta} \right) \frac{\partial}{\partial r} \left(r \frac{\partial U_e}{\partial \phi} \right) \quad (\text{A42})$$

Finally, an expression needs to be found that yields the electric scalar potential U_e . For this, Eq.(A28) is used. First, from the first relation of Eq.(33), one can write

$$\sin \theta E_\phi = \frac{\partial \Phi}{\partial \phi} = \frac{\partial}{\partial \phi} \left(\frac{1}{r} \right) \frac{\partial}{\partial r} (r U_e) \quad (\text{A43})$$

Using this and Eqs.(A38)-(A40) in Eq.(A28) gives, after some simplification,

$$-k_0^2 n^2 \frac{\partial U_e}{\partial \phi} = \frac{1}{r} \frac{\partial}{\partial \phi} \frac{\partial^2}{\partial r^2} (r U_e) + \frac{\partial}{\partial \phi} \left(\frac{1}{r^2 \sin \theta} \right) \left[\frac{\partial}{\partial \theta} \left(\sin \theta \frac{\partial U_e}{\partial \theta} \right) + \frac{\partial}{\partial \phi} \left(\frac{1}{\sin \theta} \frac{\partial U_e}{\partial \phi} \right) \right] \quad (\text{A44})$$

Integrating this expression over ϕ and using the fact that $k = k_0 n$ finally gives

$$\frac{1}{r} \frac{\partial^2}{\partial r^2} (rU_e) + \left(\frac{1}{r^2 \sin \theta} \right) \frac{\partial}{\partial \theta} \left(\sin \theta \frac{\partial U_e}{\partial \theta} \right) + \left(\frac{1}{r^2 \sin^2 \theta} \right) \left(\frac{\partial^2 U_e}{\partial \phi^2} \right) + k^2 U_e = 0 \quad (\text{A45})$$

This is the wave equation in spherical coordinates for the scalar potential of TM waves. The solution of this equation with the appropriate boundary conditions yields, from Eqs.(A38) – (A42), the components of the \vec{E} and \vec{H} fields in the case where $H_r = 0$.

Finally, through the use of Eq.(A45), Eq.(A40) for E_r can be simplified. Multiplying Eq.(A40) by $1/r$, adding it to Eq.(45) and solving for E_r gives

$$E_r = \frac{\partial^2}{\partial r^2} (rU_e) + k^2 (rU_e) \quad (\text{A46})$$

The boundary conditions for the potential U_e on a spherical surface follow from the requirement of continuity of the tangential components of the fields. For a spherical layer of radius a separating two electrically distinct regions 1 and 2, one has for the tangential component of the electric field must be continuous across the interface, i.e.,

$$E_{\theta_1}(r) \Big|_{r=a} = E_{\theta_2}(r) \Big|_{r=a} \quad (\text{A47})$$

Using Eq.(A41), this requires

$$\frac{\partial (rU_{e_1}(r))}{\partial r} \Big|_{r=a} = \frac{\partial (rU_{e_2}(r))}{\partial r} \Big|_{r=a} \quad (\text{A48})$$

i.e., the quantity $\frac{\partial (rU_e)}{\partial r}$ must be continuous across the interface. Similarly, for the magnetic field

$$H_{\phi_1}(r) \Big|_{r=a} = H_{\phi_2}(r) \Big|_{r=a} \quad (\text{A49})$$

From Eq.(A38),

$$\left(n_1^2 U_{e_1}(r) \right) \Big|_{r=a} = \left(n_2^2 U_{e_2}(r) \right) \Big|_{r=a} \quad (\text{A50})$$

across the interface.

Appendix B

Solution of the Wave Equation for the Scalar Potential in Spherical Coordinates

In this Appendix, the well-known solution of Eq.(A45) will be reviewed for completeness. Hence, solutions and boundary conditions for the potential U_e will be found from the equation

$$\frac{1}{r} \frac{\partial^2}{\partial r^2} (rU_e) + \left(\frac{1}{r^2 \sin \theta} \right) \frac{\partial}{\partial \theta} \left(\sin \theta \frac{\partial U_e}{\partial \theta} \right) + \left(\frac{1}{r^2 \sin^2 \theta} \right) \left(\frac{\partial^2 U_e}{\partial \phi^2} \right) + k^2 U_e = 0 \quad (\text{B1})$$

To this end, it is necessary to isolate terms with separate radial and angular dependencies. Multiplying Eq.(B1) through by r^2 gives

$$r \frac{\partial^2}{\partial r^2} (rU_e) + r^2 k^2 U_e + \left(\frac{1}{\sin \theta} \right) \frac{\partial}{\partial \theta} \left(\sin \theta \frac{\partial U_e}{\partial \theta} \right) + \left(\frac{1}{\sin^2 \theta} \right) \left(\frac{\partial^2 U_e}{\partial \phi^2} \right) = 0 \quad (\text{B2})$$

The form that this relation assumes suggests that one consider a solution of the multiplicative form

$$U_e = U_e(r, \theta, \phi) = R(r)Y(\theta, \phi) \quad (\text{B3})$$

Substituting Eq.(B3) into Eq.(B2) and dividing through by the same product $R(r)Y(\theta, \phi)$ yields

$$\frac{1}{R} r \frac{\partial^2}{\partial r^2} (rR) + r^2 k^2 + \left(\frac{1}{Y} \right) \left[\frac{1}{\sin \theta} \frac{\partial}{\partial \theta} \left(\sin \theta \frac{\partial Y}{\partial \theta} \right) + \left(\frac{1}{\sin^2 \theta} \right) \frac{\partial^2 Y}{\partial \phi^2} \right] = 0 \quad (\text{B4})$$

The first two terms on the left are only functions of the radial component r and the remaining terms are functions only of the angular component θ . Since there is no functional dependency between both these groups of terms, they both must be equal to a constant which is an additive inverse for each group (since they both give a final result of zero). That is, letting λ be a constant (not the wavelength), one has

$$\frac{1}{R} r \frac{\partial^2}{\partial r^2} (rR) + r^2 k^2 = \lambda \quad (\text{B5})$$

$$\left(\frac{1}{Y} \right) \left[\frac{1}{\sin \theta} \frac{\partial}{\partial \theta} \left(\sin \theta \frac{\partial Y}{\partial \theta} \right) + \left(\frac{1}{\sin^2 \theta} \right) \frac{\partial^2 Y}{\partial \phi^2} \right] = -\lambda \quad (\text{B6})$$

These relations reduce to

$$\frac{1}{r} \frac{\partial^2}{\partial r^2} (rR) + \left(k^2 - \frac{\lambda}{r^2} \right) R = 0 \quad (\text{B7})$$

$$\frac{1}{\sin \theta} \frac{\partial}{\partial \theta} \left(\sin \theta \frac{\partial Y}{\partial \theta} \right) + \left(\frac{1}{\sin^2 \theta} \right) \frac{\partial^2 Y}{\partial \phi^2} + \lambda Y = 0 \quad (\text{B8})$$

Equation (B7) gives a differential equation governing the radial function $R(r)$ of the solution. Equation (B8) can be reduced further following the same procedure as employed above. Multiplying Eq.(B8) by $\sin^2 \theta$ gives the separable relation

$$\sin \theta \frac{\partial}{\partial \theta} \left(\sin \theta \frac{\partial Y}{\partial \theta} \right) + \frac{\partial^2 Y}{\partial \phi^2} + \lambda Y \sin^2 \theta = 0 \quad (\text{B9})$$

Assuming that one can write the solution for this equation in the form

$$Y = Y(\theta, \phi) = \Theta(\theta)\Phi(\phi) \quad (\text{B10})$$

and using this in Eq.(B9) gives

$$\left(\frac{1}{\Theta} \right) \sin \theta \frac{\partial}{\partial \theta} \left(\sin \theta \frac{\partial \Theta}{\partial \theta} \right) + \lambda \sin^2 \theta = \nu \quad (\text{B11})$$

$$\left(\frac{1}{\Phi} \right) \frac{\partial^2 \Phi}{\partial \phi^2} = -\nu \quad (\text{B12})$$

These relations reduce to the governing differential equations for the colatitude function $\Theta(\theta)$ of the solution and the azimuthal function $\Phi(\phi)$, viz.,

$$\frac{1}{\sin \theta} \frac{\partial}{\partial \theta} \left(\sin \theta \frac{\partial \Theta}{\partial \theta} \right) + \left(\lambda - \frac{\nu}{\sin^2 \theta} \right) \Theta = 0 \quad (\text{B13})$$

$$\frac{\partial^2 \Phi}{\partial \phi^2} + \nu \Phi = 0 \quad (\text{B14})$$

The analysis of Eqs.(B7), (B13), and (B14), the solutions of which collectively give the composite solution of Eqs.(B3) and (B10), commences with Eq.(B14). Its solution is simply given by

$$\Phi(\phi) = A \exp(i\sqrt{\nu}\phi) + B \exp(-i\sqrt{\nu}\phi) \quad \nu \neq 0 \quad (\text{B15})$$

$$\Phi(\phi) = A + B\phi, \quad \nu = 0 \quad (\text{B16})$$

Since the propagation problem addressed here does not involve the azimuthal coordinate ϕ , $\nu = 0$; additionally, since no particular value for ϕ is specified, $B = 0$, and thus

$$\Phi(\phi) = A = \text{const.} \quad (\text{B17})$$

Equation (B13) now becomes

$$\frac{1}{\sin \theta} \frac{\partial}{\partial \theta} \left(\sin \theta \frac{\partial \Theta}{\partial \theta} \right) + \lambda \Theta = 0 \quad (\text{B18})$$

Changing variables to $w \equiv -\cos \theta$, Eq.(B18) takes the form

$$\frac{d}{dw} \left[(1-w^2) \frac{dP(w)}{dw} \right] + \lambda P(w) = 0 \quad (\text{B19})$$

where

$$\Theta(\theta) = P(-\cos \theta) = P(w) \quad (\text{B20})$$

(The choice of $w = \cos \theta$ would also be acceptable and indeed is the most popular one. However, employing Eq.(B20) allows the solution to be regular at $\theta = \pi$ and to contain a singularity at $\theta = 0$; this property will be essential when matching source boundary conditions to the problem.) The solution to Eq.(B19) will be taken to be given by the infinite series in w , i.e.,

$$P(w) = \sum_{j=0}^{\infty} a_j w^j \quad (\text{B21})$$

which gives, upon substitution into Eq.(B19),

$$\sum_{j=0}^{\infty} (j+2)(j+1) a_{j+2} w^j - \sum_{j=0}^{\infty} j(j+1) a_j w^j + \lambda \sum_{j=0}^{\infty} a_j w^j = 0 \quad (\text{B22})$$

Since this relation must hold for every power of w , the coefficient separately must satisfy

$$(j+2)(j+1) a_{j+2} - j(j+1) a_j + \lambda a_j = 0 \quad (\text{B23})$$

Solving this equation for a_{j+2} yields

$$a_{j+2} = \frac{j(j+1) - \lambda}{(j+2)(j+1)} a_j \quad (\text{B24})$$

If the series given by Eq.(B21) does not terminate at some value for j , it is seen from Eq.(B24) that

$$\lim_{j \rightarrow \infty} \frac{a_{j+2}}{a_j} = \frac{j}{j+2} \quad (\text{B25})$$

At the values of $w = \pm 1$, the series will diverge. This is not an acceptable situation for a physically realizable situation. Thus, the series must terminate at some value of j , e.g., $j = l$. From Eq.(B24), with $a_{l+2} = 0$ (i.e., the series terminates), one must have

$$\lambda = l(l+1) \quad (\text{B26})$$

where l is a positive integer. This is the fundamental source of the combination $l(l+1)$ throughout the equations of propagation involving the angular coordinate θ . Therefore, Eq.(B19) becomes

$$\frac{d}{dw} \left[(1-w^2) \frac{dP_l(w)}{dw} \right] + l(l+1)P_l(w) = 0 \quad (\text{B27})$$

in which $P_l(w)$ is now also a function of l . This differential equation defines [1] the Legendre functions $P_l(w)$.

To find explicit expressions for the functions $P_l(w)$, consider another change of variables, i.e.,

$$\nu = (w^2 - 1)^l \quad (\text{B28})$$

Equation (B27) then simplifies to

$$(1-w^2) \frac{d\nu}{dw} + 2l\nu = 0 \quad (\text{B29})$$

Differentiating this relation with respect to w $j+1$ times gives

$$(1-w^2) \frac{d^2 t}{dw^2} - (2j-2l+2)w \frac{dt}{dw} + (2l-j)(j+1)t = 0 \quad (\text{B30})$$

where

$$t \equiv \frac{d^j \nu}{dw^j} = \frac{d^j}{dw^j} (w^2 - 1)^l \quad (\text{B31})$$

At the specific value of $j = l$, Eq.(B30) yields

$$(1-w^2)\frac{d^2t}{dw^2}-2w\frac{dt}{dw}+l(l+1)t=0 \quad (\text{B32})$$

which is Eq.(B27) for $t = P_l(w)$. At $j = l$, Eq.(B31) differs only by a constant factor. Thus, at the outset, setting $P_l(1)=1$ for all l finally gives

$$P_l(w)=\frac{1}{2^l l!}\frac{d^l}{dw^l}(w^2-1)^l \quad (\text{B33})$$

The first three Legendre functions are thus given by

$$P_0(w)=1 \quad (\text{B34})$$

$$P_1(w)=w=-\cos\theta \quad (\text{B35})$$

$$P_2(w)=\frac{1}{2}(3w^2-1)=\frac{1}{2}(3\cos^2\theta-1) \quad (\text{B36})$$

The analysis of Eq.(B7) can proceed in one of two ways. First, it must be noted that like that of the function $P_l(w)$, the radial function now also becomes a function of l upon use of Eq.(B26), i.e., $R(r)=R_l(r)$. In the first approach to Eq.(B7), one can simply expand the second derivative with respect to r and obtain

$$\frac{d^2R_l}{dr^2}+\frac{2}{r}\frac{dR_l}{dr}+\left(k^2-\frac{l(l+1)}{r^2}\right)R_l=0 \quad (\text{B37})$$

Solutions to this equation are linear combinations of spherical Bessel Functions [2,3] of the first kind $j_l(kr)$ and of the second kind $n_l(kr)$, i.e.,

$$R_l(r)=Aj_l(kr)+Bn_l(kr) \quad (\text{B38})$$

where the constants A and B are determined by the boundary conditions of the problem. The analysis of these functions can be carried out in an analogous manner to that of Eq.(B19); see, e.g., [3] for details.

Hence, for the propagation problem addressed in this work, the solution of Eq.(B1) is given by Eqs.(B3), (B10), (B17), and (B20), viz,

$$U_e(r,\theta)=R_l(r)P_l(-\cos\theta) \quad (\text{B39})$$

or some linear combination of this composite function, adhering to some prevailing boundary and source conditions.

A second approach using Eq.(B7) in terrestrial propagation scenarios involves the use of a transformation and an approximation. First, the transformation simply involves the prescription

$$\tilde{R}_l(r) = rR_l(r) \quad (\text{B40})$$

allowing Eq.(B7) to become

$$\frac{d^2 \tilde{R}_l}{dr^2} + \left(k^2 - \frac{l(l+1)}{r^2} \right) \tilde{R}_l = 0 \quad (\text{B41})$$

The general solution of Eq.(B39) now becomes in terms of the radial function $\tilde{R}_l(r)$

$$U_e(r, \theta) = C \frac{\tilde{R}_l(r)}{r} P_l(-\cos \theta) \quad (\text{B42})$$

Using the solution of Eq.(B41) is, remembering Eqs.(B38) and (B40),

$$\tilde{R}_l(r) = r [A_j_l(kr) + B n_l(kr)] \quad (\text{B43})$$

from which, using Eq.(B42), leads back to Eq.(B39). The point here is that the form of Eq.(B41) is amenable to approximations which give solutions that differ from Eq.(B43). This form of the radial equation is used in this work because of this flexibility. An example of such an approximate solution will now be given.

Application of Eq.(B41) to a terrestrial propagation problem above the surface of a planet of radius a is as follows. Letting ξ be the distance above the surface, one has $r = a + \xi$, where, in general, $\xi \ll a$. In this instance, one can approximately write

$$\frac{1}{r^2} = (a + \xi)^{-2} = a^{-2} \left(1 + \frac{\xi}{a} \right)^{-2} \approx a^{-2} \left(1 - 2 \frac{\xi}{a} \right) \quad (\text{B44})$$

Using this in Eq.(B41) and changing variables from r to ξ yields

$$\frac{d^2 \tilde{R}_l(\xi)}{d\xi^2} + \left(k^2 - \frac{l(l+1)}{a^2} + \frac{2l(l+1)}{a^3} \xi \right) \tilde{R}_l(\xi) = 0 \quad (\text{B45})$$

Changing variables once again using

$$\zeta \equiv \left(\frac{2l(l+1)}{a^3} \right)^{1/3} \xi \quad (\text{B46})$$

finally gives

$$\frac{d^2 \tilde{R}_l(\zeta)}{d\zeta^2} + \left[\left(k^2 - \frac{l(l+1)}{a^2} \right) \left(\frac{a^3}{2l(l+1)} \right)^{2/3} + \zeta \right] \tilde{R}_l(\zeta) = 0 \quad (\text{B47})$$

Letting

$$t_l \equiv - \left(k^2 - \frac{l(l+1)}{a^2} \right) \left(\frac{a^3}{2l(l+1)} \right)^{2/3} \quad (\text{B48})$$

Eq.(B47) can be written as

$$\frac{d^2 \tilde{R}_l(\zeta)}{d\zeta^2} - [t_l - \zeta] \tilde{R}_l(\zeta) = 0 \quad (\text{B49})$$

the solution of which are Airy functions [4]. This form of the radial equation was extensively employed by Fock [5] in early investigations of radio wave propagation above the Earth's surface; see also [6]. The specific values of t_l are determined by the prevailing boundary conditions.

Finally, the expressions for the boundary conditions for the tangential electric and magnetic field discussed in Appendix I, (Eqs.(A48) and (A50)) can be expanded upon. Equation (A48) for the continuity of the tangential electric field across a boundary at $r = a$ separating regions 1 and 2 becomes, using Eq.(B42),

$$\left. \frac{\partial \tilde{R}_{l,1}}{\partial r} \right|_{r=a} = \left. \frac{\partial \tilde{R}_{l,2}}{\partial r} \right|_{r=a} \quad (\text{B50})$$

Similarly, Eq.(A50) for the continuity of the tangential magnetic field across the boundary becomes

$$n_1^2 \tilde{R}_{l,1} \Big|_{r=a} = n_2^2 \tilde{R}_{l,2} \Big|_{r=a} \quad (\text{B51})$$

References for Appendix B

1. M. Abramowitz and I. A. Stegun, eds., *Handbook of Mathematical Functions* (Dover, New York, 1972), p. 332.
2. Ref. 1, p. 437.
3. G. Arfkin, *Mathematical Methods for Physicists*, 3rd Ed. (Academic Press, New York, 1985), Chapt. 11.
4. Ref. 1, p. 446.
5. V. A. Fock, *Electromagnetic Diffraction and Propagation Problems* (Pergamon Press, New York, 1965), Chapt. 12.
6. J. Galejs, *Terrestrial Propagation of Long Electromagnetic Waves* (Pergamon Press, New York, 1972), pp. 105-107.

REPORT DOCUMENTATION PAGE

Form Approved
OMB No. 0704-0188

The public reporting burden for this collection of information is estimated to average 1 hour per response, including the time for reviewing instructions, searching existing data sources, gathering and maintaining the data needed, and completing and reviewing the collection of information. Send comments regarding this burden estimate or any other aspect of this collection of information, including suggestions for reducing this burden, to Department of Defense, Washington Headquarters Services, Directorate for Information Operations and Reports (0704-0188), 1215 Jefferson Davis Highway, Suite 1204, Arlington, VA 22202-4302. Respondents should be aware that notwithstanding any other provision of law, no person shall be subject to any penalty for failing to comply with a collection of information if it does not display a currently valid OMB control number.

PLEASE DO NOT RETURN YOUR FORM TO THE ABOVE ADDRESS.

1. REPORT DATE (DD-MM-YYYY) 01-10-2008		2. REPORT TYPE Technical Memorandum		3. DATES COVERED (From - To)	
4. TITLE AND SUBTITLE Long-Range Transhorizon Lunar Surface Radio Wave Propagation in the Presence of a Regolith and a Sparse Exospheric Plasma				5a. CONTRACT NUMBER	
				5b. GRANT NUMBER	
				5c. PROGRAM ELEMENT NUMBER	
6. AUTHOR(S) Manning, Robert, M.				5d. PROJECT NUMBER	
				5e. TASK NUMBER	
				5f. WORK UNIT NUMBER WBS 903184.04.03.02.01	
7. PERFORMING ORGANIZATION NAME(S) AND ADDRESS(ES) National Aeronautics and Space Administration John H. Glenn Research Center at Lewis Field Cleveland, Ohio 44135-3191				8. PERFORMING ORGANIZATION REPORT NUMBER E-16680	
9. SPONSORING/MONITORING AGENCY NAME(S) AND ADDRESS(ES) National Aeronautics and Space Administration Washington, DC 20546-0001				10. SPONSORING/MONITORS ACRONYM(S) NASA	
				11. SPONSORING/MONITORING REPORT NUMBER NASA/TM-2008-215463	
12. DISTRIBUTION/AVAILABILITY STATEMENT Unclassified-Unlimited Subject Categories: 17, 32, and 91 Available electronically at http://gltrs.grc.nasa.gov This publication is available from the NASA Center for AeroSpace Information, 301-621-0390					
13. SUPPLEMENTARY NOTES					
14. ABSTRACT Long-range, over-the-horizon (transhorizon) radio wave propagation is considered for the case of the Moon. In the event that relay satellites are not available or otherwise unwarranted for use, transhorizon communication provides for a contingency or backup option for non line-of-sight lunar surface exploration scenarios. Two potential low-frequency propagation mechanisms characteristic of the lunar landscape are the lunar regolith and the photoelectron induced plasma exosphere enveloping the Moon. Although it was hoped that the regolith would provide for a spherical waveguide which could support a trapped surface wave phenomena, it is found that, in most cases, the regolith is deleterious to long range radio wave propagation. However, the presence of the plasma of the lunar exosphere supports wave propagation and, in fact, surpasses the attenuation of the regolith. Given the models of the regolith and exosphere adopted here, it is recommended that a frequency of 1 MHz be considered for low rate data transmission along the lunar surface. It is also recommended that further research be done to capture the descriptive physics of the regolith and the exospheric plasma so that a more complete model can be obtained. This comprehensive theoretical study is based entirely on first principles and the mathematical techniques needed are developed as required; it is self-contained and should not require the use of outside resources for its understanding.					
15. SUBJECT TERMS Radio waves; Radio transmission; Wave propagation; Moon					
16. SECURITY CLASSIFICATION OF:			17. LIMITATION OF ABSTRACT	18. NUMBER OF PAGES	19a. NAME OF RESPONSIBLE PERSON
a. REPORT	b. ABSTRACT	c. THIS PAGE			STI Help Desk (email:help@sti.nasa.gov)
U	U	U	UU	61	19b. TELEPHONE NUMBER (include area code) 301-621-0390

